UNIVERSITY OF CALIFORNIA,
IRVINE

Progress Towards the Development of a Covalently Binding TLR 7/8 Agonist

THESIS

submitted in partial satisfaction of the requirements
for the degree of

MASTER OF SCIENCE

in Chemistry

by

Alfred C. Chon

Thesis Committee:
Associate Professor Aaron Esser-Kahn, Chair
Associate Professor Jennifer Prescher
Professor Kenneth Shea

2017

DEDICATION

To

my mother

for being the toughest person I know.

TABLE OF CONTENTS

LIST OF FIGURES

LIST OF SCHEMES

LIST OF TABLES

ACKNOWLEDGMENTS

I would first like to thank my committee chair, Professor Aaron Esser-Kahn. I would not be where I am now without him. He has challenged me to go outside my comfort zone to continually grow and learn as a scientist. But beyond the lessons in science and in research, he has always been very open and candid, qualities that I have come to appreciate!

Next, I would like to thank my committee members, Professor Jennifer Prescher and Professor Kenneth Shea for all the time and support they have given me.

I would also like to thank our funding source, the NIH. Additionally, I would like to thank the Department of Education for supporting me through the Graduate Assistance in Areas of National Need (GAANN) fellowship.

I would like to thank Geoffrey Lynn (NIH) for his assistance in performing the *in vivo* and *ex vivo* work. Additionally, I would like to thank Misako Matsumoto for providing the TLR8-FLAG plasmid.

Of course, I must thank all of the Esser-Kahn lab, for without them I would not have had nearly as much fun. To Janine Tom, you were my partner in synthesis, music, and food. To Arvind Bhattacharya, my first undergrad, you taught me what it means to be a mentor and educate others.

ABSTRACT OF THE THESIS

Progress Towards the Development of a Covalently Binding TLR 7/8 Agonist

By

Alfred C. Chon

Master of Science in Chemistry

University of California, Irvine, 2017

Associate Professor Aaron Esser-Kahn, Chair

The agonists of Toll-like receptors (TLRs) are interesting targets for vaccine adjuvants and other immunotherapies. One particular challenge in their use is their poor pharmacokinetic properties. Targeted covalent inhibitors have been shown to have irreversible binding with the receptors of interest, leading to high selectivity and potency. These properties are very attractive for TLR agonists. In addition, it is currently not known what effect continuous activation of TLRs will have on immune activation. Drawing inspiration from ligand-directed tosyl chemistry, we have synthesized several potential covalent agonists of TLR 7/8 and evaluated them in biological assays. Additionally, we have made progress in determining if these agonists do indeed proceed through covalent modification of the receptor.

Chapter 1

Introduction

1.1 Motivation

The prevention of disease and death through vaccination is one of the greatest achievements of 20th century.[1,2] By administering a weakened version or pieces of a pathogen, vaccines engage the host's immune system toward a target pathogen, leading to protection.[3,4] Advances have been made in developing alternative preparations of pathogens for administration in vaccines.[2] However, there are still challenges with low immunogenicity, resulting in decreased efficacy. In addition, most vaccines have been developed empirically, with little knowledge of their mechanism of action. As a result, there are still many diseases, like malaria, HIV, and Zika, for which there are no effective vaccines.

In order to address the challenges of efficacy, vaccines have been formulated with the use of adjuvants to elicit an enhanced immune response during vaccination.[2,4,5] Adjuvants are substances that enhance the host's response to a co-administered antigen by directing the immune response. Increased understanding of the innate immune system's response has led to the development of improved adjuvants.[5] In the Esser-Kahn lab, we are interested in better understanding the response of the innate immune system through the use of synthetic chemical tools.[6,7] It is known that stimulation of different immune receptors results in different immune responses.[5] However, it is unknown if different immune responses can be achieved from the same immune receptor by manipulating the stimulation event. Using chemical synthesis, we can develop agonists to immune receptors that bind differently from the native agonists to manipulate the immune response.

1.2 The Immune System and Pattern Recognition Receptors

When a pathogen attacks a host, there is a rapid and long-term immune response, elicited by the host's innate and adaptive immune systems, respectively (**Figure 1-1**).[8] Activation of the innate immune system results in a rapid nonspecific immune response, priming an adaptive immune response against a specific antigen, eventually leading to immunity against the antigen. Increased understanding of the innate immune response has led to the development of improved adjuvants.

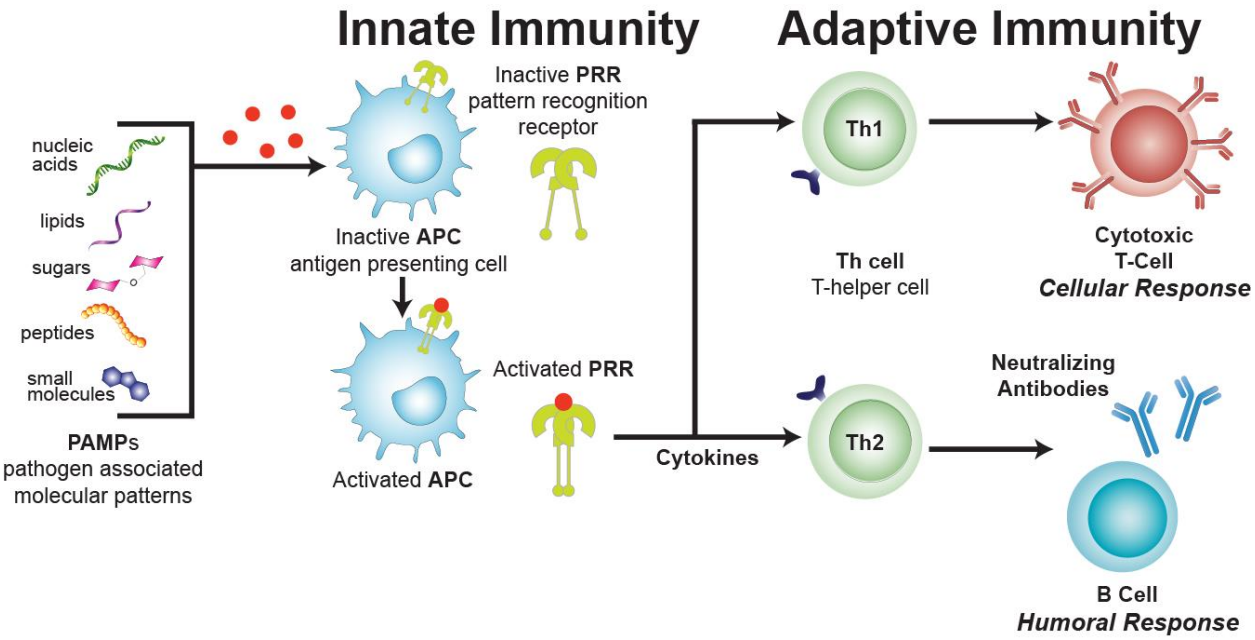

Figure 1-1: Activating the innate and adaptive immune systems and responses.

Antigen-presenting cells (APCs), such as dendritic cells and macrophages, are the major cell type of the innate immune system.[8–11] APCs express pattern recognition receptors (PRRs) that are activated by structurally conserved molecular components of pathogens, known as pathogen-associated molecular patterns (PAMPs).[5] When PRRs are activated, this leads to a response in APCs, including the activation of transcription factors, upregulation of cell surface markers, and the production of signaling cytokines. PRRs are key players in modulating and controlling immune responses, leading to efforts to explore PRR ligands as adjuvants.[5,12] PRR ligands are

diverse, ranging from small heterocyclic molecules to RNA to lipopeptides. Using chemical synthesis, we can modify these PRR ligands to study how different modifications affect the innate immune system response.

The adaptive immune system is comprised of T and B cells and maintains the body's long-term immune response, making it essential for lasting protection against pathogens. Depending on the cell surface markers and cytokines elicited by the innate immune system, the adaptive immune system can be polarized towards two distinct helper T-cell responses, Th1 and Th2, resulting in cellular and humoral or antibody responses, respectively.[5,11] In order to protect against different pathogens, distinct immune responses are necessary. Thus, by altering the innate immune system response with chemically modified PAMPs, the adaptive immune system response can be modulated, resulting in the desired immune response for protection against a particular pathogen.

1.3 Toll-like Receptors and Adjuvants

Toll-like receptors (TLRs) are one of the best characterized and well-studied classes of PRRs.[5,13,14] TLR signaling is activated by a diverse group of PAMPs (**Figure 1-2**). Of the 10 known TLRs in human and 12 in mice, the first 9 are the most well-studied and characterized. TLRs 1, 2, 4, 5, and 6 are located on the cell surface and TLRs 3, 7, 8, and 9 are in the endosome. Broadly, the cellular location of the TLRs dictates the type of PAMP recognized: cell surface TLRs recognize bacterial cell wall components (lipids, lipopeptides, and proteins) and endosomal TLRs bind to pathogen-derived nucleic acids (ssDNA, ssRNA, and dsRNA).[15] Activation of different TLRs results in a distinct immune response.

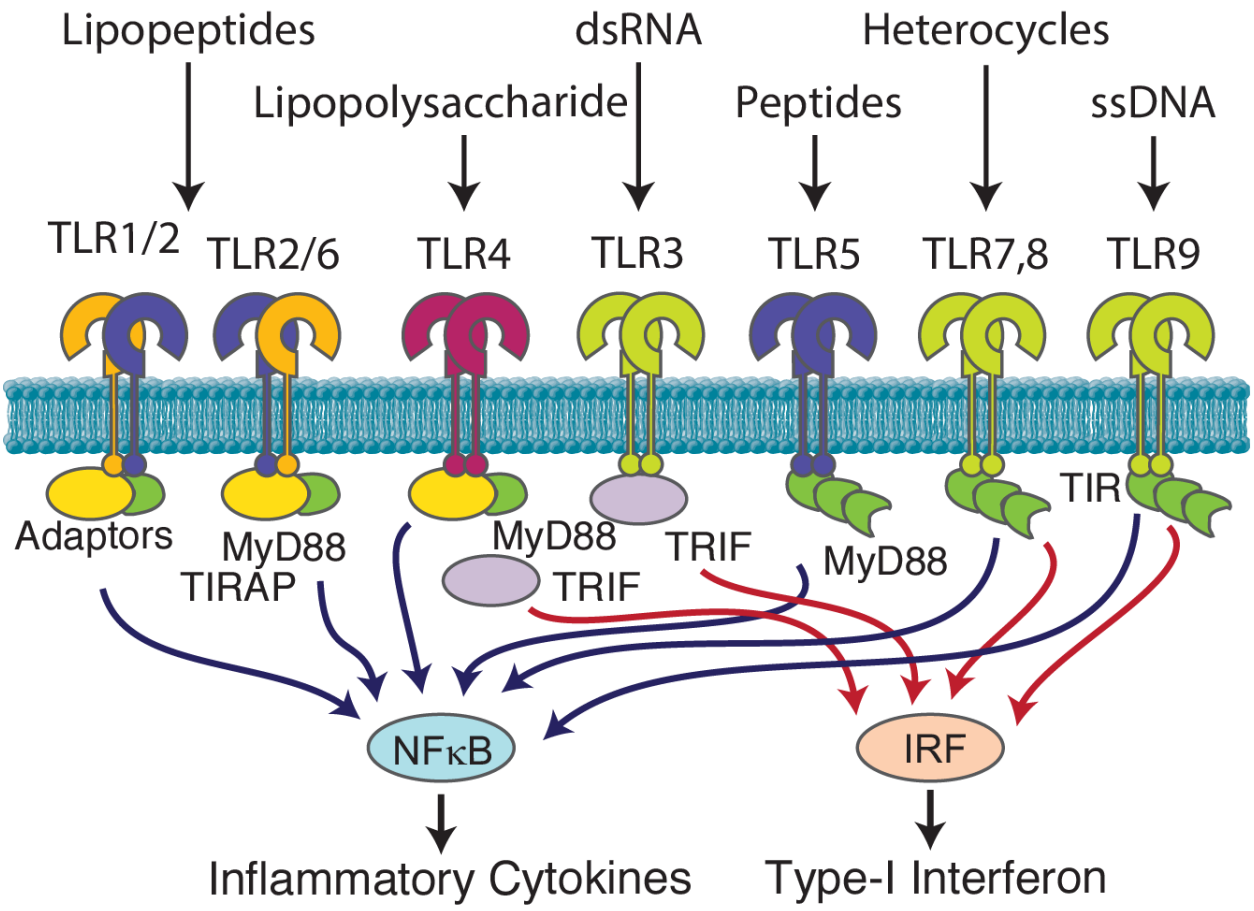

Figure 1-2: Toll-like receptors (TLRs), their agonists, and their signaling pathways.

Due to their distinct immune response, TLR agonists have been identified as promising targets for the development of new vaccine adjuvants.[5,16] An agonist of TLR4, monophosphoryl lipid A, has become the first adjuvant approved for use in vaccine formulation by the FDA.[17] Despite the diversity of agonists, activation of TLRs tends to result in a strong Th1 response.[5] In order to achieve complete protection against a wide variety of pathogens, it is necessary to be able to tune the immune response for the pathogen of interest.

While some TLR agonists, including flagellin (TLR5 agonist), imidazoquinolines (TLR7 agonist), and CpG-DNA (TLR9), are currently being tested in clinical trials due to their ability to induce immune reactions, many agonists exhibit poor pharmacokinetic properties, resulting in

the underachievement of TLR agonists in the clinic.[18–20] The therapeutic efficacy of TLR agonists is hindered by their short half-life. In addition, due to the widespread distribution of these agonists *in vivo*, negative system effects are seen, limiting the dose and the agonists' effect on the microenvironment of interest.[18] In order for TLR agonists to be effective vaccine adjuvants, these properties must be addressed.

1.4 Irreversible Covalently Binding Ligands

One strategy to address these issues with pharmacokinetic properties is to synthesize irreversible covalently binding ligands or covalent ligands. In comparison to typical ligands, which are in equilibrium with their receptor target, continually binding, un-binding, and rebinding, covalent ligands form a permanent, covalent bond.[21] Most commonly, this strategy has been used to develop targeted covalent inhibitors.

Targeted covalent inhibitors leverage the formation of a covalent bond to increase potency, selectivity, and receptor occupancy.[21,22] Low molecular weight molecules typically have low potencies, but covalent binding allow for high potency with all the benefits associated with lower molecular weights. In the design of targeted covalent inhibitors, a specific nucleophile that is unique or rare across a protein family is targeted. This ensures that the inhibitor cannot form a covalent bond with most family members of the protein of interest, increasing selectivity. The covalent bond also requires that the protein target is re-synthesized to restore activity, resulting in increased receptor occupancy. These are all properties that would be desirable for the small molecule TLR agonists, including imidazoquinolines.

1.5 This Work

Despite the application of TLR agonists as potential vaccine adjuvants, many candidates have been affected by poor pharmacokinetic properties. The synthesis of covalently binding TLR agonists could address these issues. There have been no previous reports of covalently binding TLR agonists. Therefore, we are also interested in studying what effects covalent binding will have on immune activity. Herein, we report and discuss our progress on synthesizing and evaluating potential covalent TLR agonists, as well as confirming their mechanism of action.

1.6 References

(1) Bärnighausen, T.; Bloom, D. E.; Cafiero-Fonseca, E. T.; O'Brien, J. C. Valuing Vaccination. *Proc. Natl. Acad. Sci.* **2014**, *111* (34), 12313–12319.

(2) WHO | State of the world's vaccines and immunization. Third edition http://who.int/immunization/sowvi/en/ (accessed Sep 8, 2017).

(3) Plotkin, S. History of Vaccination. *Proc. Natl. Acad. Sci.* **2014**, *111* (34), 12283–12287.

(4) De Gregorio, E.; Rappuoli, R. From Empiricism to Rational Design: A Personal Perspective of the Evolution of Vaccine Development. *Nat. Rev. Immunol.* **2014**, *14* (7), 505–514.

(5) Maisonneuve, C.; Bertholet, S.; Philpott, D. J.; Gregorio, E. D. Unleashing the Potential of NOD- and Toll-like Agonists as Vaccine Adjuvants. *Proc. Natl. Acad. Sci.* **2014**, *111* (34), 12294–12299.

(6) Ryu, K. A.; Stutts, L.; Tom, J. K.; Mancini, R. J.; Esser-Kahn, A. P. Stimulation of Innate Immune Cells by Light-Activated TLR7/8 Agonists. *J. Am. Chem. Soc.* **2014**, *136* (31), 10823–10825.

(7) Tom, J. K.; Dotsey, E. Y.; Wong, H. Y.; Stutts, L.; Moore, T.; Davies, D. H.; Felgner, P. L.; Esser-Kahn, A. P. Modulation of Innate Immune Responses via Covalently Linked TLR Agonists. *ACS Cent. Sci.* **2015**, *1* (8), 439–448.

(8) Medzhitov, R.; Janeway, C. A. Innate Immunity: Impact on the Adaptive Immune Response. *Curr. Opin. Immunol.* **1997**, *9* (1), 4–9.

(9) Janeway, C. A.; Medzhitov, R. Innate Immune Recognition. *Annu. Rev. Immunol.* **2002**, *20*, 197–216.

(10) Hoebe, K.; Janssen, E.; Beutler, B. The Interface between Innate and Adaptive Immunity. *Nat. Immunol.* **2004**, *5* (10), 971–974.

(11) Iwasaki, A.; Medzhitov, R. Control of Adaptive Immunity by the Innate Immune System. *Nat. Immunol.* **2015**, *16* (4), 343–353.

(12) Bergmann-Leitner, E. S.; Leitner, W. W. Adjuvants in the Driver's Seat: How Magnitude, Type, Fine Specificity and Longevity of Immune Responses Are Driven by Distinct Classes of Immune Potentiators. *Vaccines* **2014**, *2* (2), 252–296.

(13) Beutler, B. A. TLRs and Innate Immunity. *Blood* **2009**, *113* (7), 1399–1407.

(14) Akira, S.; Takeda, K. Toll-like Receptor Signalling. *Nat. Rev. Immunol.* **2004**, *4* (7), 499–511.

(15) Barton, G. M.; Kagan, J. C. A Cell Biological View of Toll-like Receptor Function: Regulation through Compartmentalization. *Nat. Rev. Immunol.* **2009**, *9* (8), 535–542.

(16) Hedayat, M.; Takeda, K.; Rezaei, N. Prophylactic and Therapeutic Implications of Toll-like Receptor Ligands. *Med. Res. Rev.* **2012**, *32* (2), 294–325.

(17) Mata-Haro, V.; Cekic, C.; Martin, M.; Chilton, P. M.; Casella, C. R.; Mitchell, T. C. The Vaccine Adjuvant Monophosphoryl Lipid A as a TRIF-Biased Agonist of TLR4. *Science* **2007**, *316* (5831), 1628–1632.

(18) Engel, A. L.; Holt, G. E.; Lu, H. The Pharmacokinetics of Toll-like Receptor Agonists and the Impact on the Immune System. *Expert Rev. Clin. Pharmacol.* **2011**, *4* (2), 275–289.

(19) Reed, S. G.; Bertholet, S.; Coler, R. N.; Friede, M. New Horizons in Adjuvants for Vaccine Development. *Trends Immunol.* **2009**, *30* (1), 23–32.

(20) Hennessy, E. J.; Parker, A. E.; O'Neill, L. A. J. Targeting Toll-like Receptors: Emerging Therapeutics? *Nat Rev Drug Discov* **2010**, *9* (4), 293–307.

(21) Singh, J.; Petter, R. C.; Baillie, T. A.; Whitty, A. The Resurgence of Covalent Drugs. *Nat Rev Drug Discov* **2011**, *10* (4), 307–317.

(22) Smith, A. J. T.; Zhang, X.; Leach, A. G.; Houk, K. N. Beyond Picomolar Affinities: Quantitative Aspects of Noncovalent and Covalent Binding of Drugs to Proteins. *J. Med. Chem.* **2009**, *52* (2), 225–233.

Chapter 2

Synthesis and Evaluation of Covalent Imidazoquinolines

2.1 Design of Covalent TLR Agonist

To synthesize a covalent TLR agonist, we wished to use a TLR agonist that was a small molecule and had a crystal structure of agonist binding with the receptor. The imidazoquinoline class of TLR 7/8 agonists satisfied both of these conditions (**Figure 2-1A**).[1] Additionally, there was precedence for how different structural modifications of imidazoquinolines affect immune activity.[2,3]

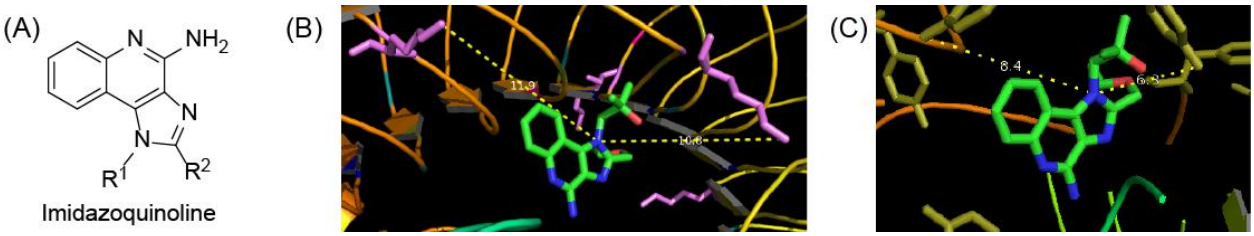

Figure 2-1: (A) General structure of the imidazoquinolines class of TLR 7/8 agonists. **(B)** Lysines found in ligand binding pocket. **(C)** Tyrosines found in ligand binding pocket.

Drawing inspiration from the targeted covalent inhibitors, we examined the available crystal structures of resiquimod, an imidazoquinoline analog, bound to TLR8 to determine if there was a cysteine in the binding pocket.[1] This would then allow for the use of a Michael acceptor to generate the covalent TLR agonist. Unfortunately, there were no cysteines found in the binding pocket. We then examined the binding pocket to see if there were any other nucleophilic amino acid residues. We identified several lysines and tyrosines in the binding pocket (**Figure 2-1B,C**). Instead of a Michael addition approach, these residues could be used with a ligand-directed tosyl (LDT) chemistry approach.

LDT has been used for the site-selective attachment of synthetic probes on to endogenous proteins *in vivo* and *in vitro*.[4–7] In the attachment of synthetic probes into specific proteins, LDT has the advantage of not requiring genetic modification of the protein. In this approach, the ligand non-covalently binds to the target protein, which results in a proximity driven substitution reaction with a reactive nucleophilic amino acid residue in the binding pocket to displace the internal sulfonate (**Figure 2-2A**). LDT is usually used to covalently attach synthetic probes, including fluorophore, biotin, and ^{19}F NMR probes, without covalent attachment of the ligand.

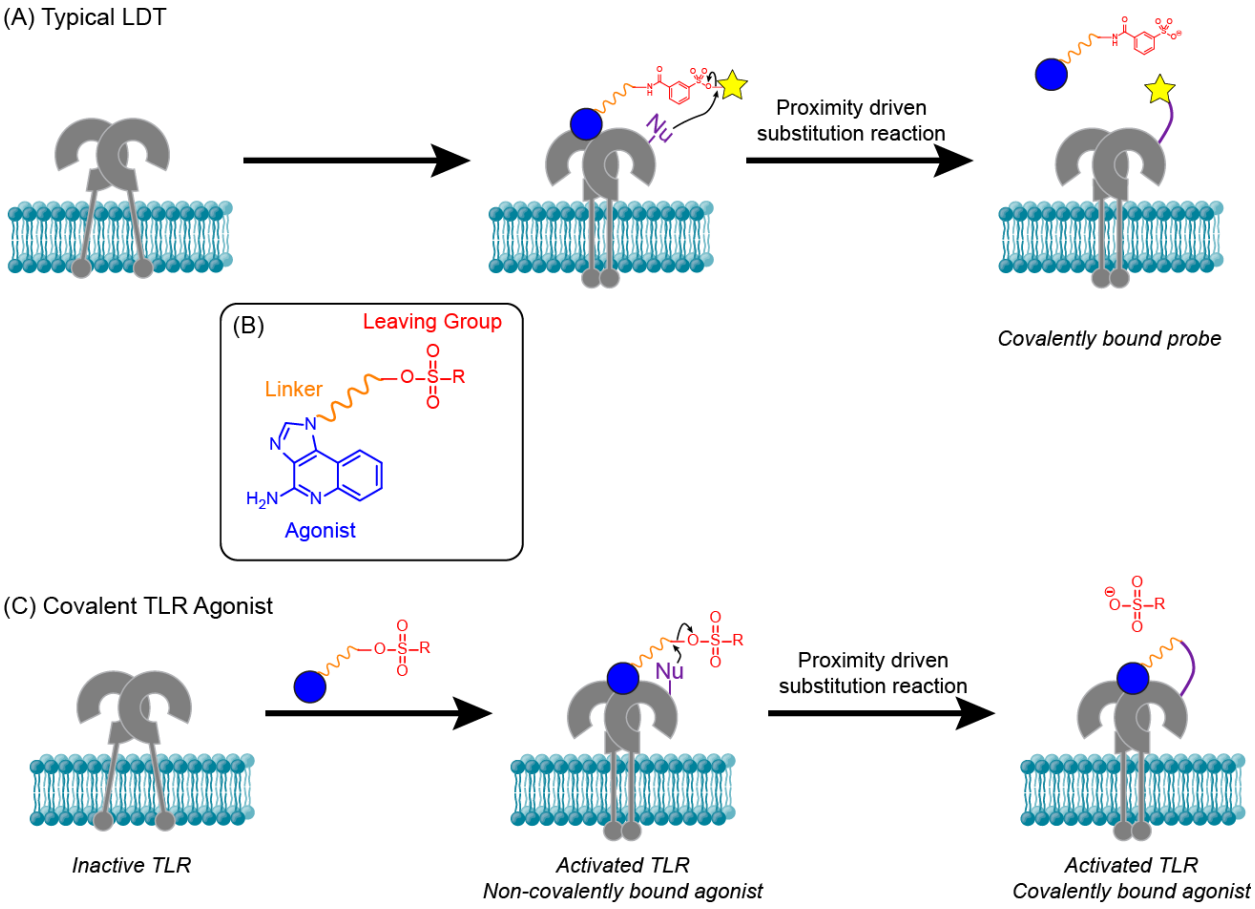

Figure 2-2: (A) Typical ligand-directed tosyl chemistry (LDT) to attach a probe (star) to a protein of interest. **(B)** General design of covalently binding imidazoquinolines agonist. **(C)** Proposed mechanism for covalent binding of imidazoquinolines to TLR inspired by LDT.

In order to adapt the LDT chemistry for our purposes, we envisioned an imidazoquinoline, with some sort of linker, with a terminal sulfonate (**Figure 2-2B**). This covalent TLR agonist would first undergo non-covalent binding with the TLR, then, by proximity driven substitution reaction, displace the sulfonate, covalently attaching the TLR agonist to the receptor (**Figure 2-2C**).

We identified three known conjugatable imidazoquinolines that we sought to modify into a covalent agonist: **2H**, **2B**, **2Bxy** (**Figure 2-3**).[8] These three imidazoquinolines have different potencies, as determined by NF-κB activity, with **2H** being the least potent and **2Bxy** being the most potent. This would allow us to see if the modification of these agonists with a tosylate affected immune activity differently depending on the activity of the parent compound.

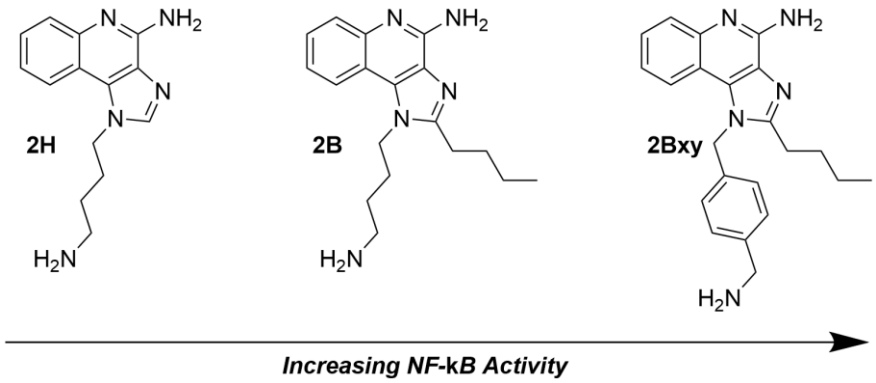

Figure 2-3: Three conjugatable imidazoquinolines of interest, arranged in order of increasing NF-**κ**B activity.

Based on the crystal structure and work by Hamachi, we would utilize a C12-alkyl linker between the imidazoquinoline and the terminal sulfonate.[1,5,6] In terms of linker type we wanted something that was flexible and easy to modify with a tosylate. Hamachi did much of their earlier work with alkyl linkers. In terms of linker length, Hamachi has pointed out that while linker length does affect the efficiency of labeling, the major requirement is being long enough to reach the residues. Thus, taking the crystal structure into consideration, we settled on a C12 linker because it provided enough length to reach the closest amino acid residues shown in

Figure 2-1B,C. The linker is certainly one aspect that should be investigated more thoroughly to achieve an optimal covalent agonist. Different linker types like PEG could certainly help with solubility and different linker lengths could allow for selective labeling of specific amino acid residues.

For the terminal sulfonate, we used a tosylate because it was convenient to synthetically access and was similar to the internal benzenesulfonates utilized by Hamachi for his LDT probes.

We could access our desired covalent TLR agonists via conjugation of the imidazoquinolines with a terminal tosylate linker with a carboxylic acid handle.

2.2 Synthesis of Imidazoquinolines

Synthesis of the conjugatable imidazoquinolines **2H**, **2B**, and **2Bxy** all started with reaction of 2,4-quinolinediol, **2.1**, with nitric acid at 75 °C to nitrate the 3-position, yielding **2.2** quantitatively (**Scheme 2-1**). The nitroquinolinediol was then chlorinated with phenylphosphonic dichloride to afford **2.3** in 81% yield.

Towards the completion of **2H** and **2B**, **2.3** was reacted with N-Boc-1,4-butanediamine in the presence of trimethylamine at 70 °C to selectively substitute the 4-chloro, resulting in **2.4** in 88% yield after trituration. The nitro-group was then reduced by high pressure hydrogenation with catalytic Pt/C yielding **2.5** in 86% yield. Towards **2H**, **2.5** was then reacted with triethyl orthoformate at 100 °C to perform the ring closure, resulting in **2.6** in 94% yield. To finish making **2H**, the 2-chloro was substituted with benzylamine at 145 °C to give **2.7** in 54% yield, followed by global deprotection in sulfuric acid to give **2H** in 62% yield. Towards **2B**, **2.5** was refluxed with trimethyl orthovalerate in the presence of pyridine hydrochloride in toluene, to yield **2.8** in 48% yield. Similarly to **2H**, **2B** was achieved by substituting **2.8** with benzylamine to

yield **2.9**, followed by subsequent global deprotection with sulfuric acid to yield **2B**, in 72% and 54% yields respectively.

Towards the completion of **2Bxy**, **2.3** was reacted with 1-(N-Boc-aminomethyl)-4-(aminomethyl)benzene in the presence of trimethylamine at 45 °C to selectively substitute the 4-chloro, resulting in **2.10** in 72% yield. **2.10** was the reduced with high pressure hydrogenation with Pt/C to yield **2.11** quantitatively. Subsequent reflux of **2.11** with trimethyl orthovalerate in the presence of pyridine hydrochloride in toluene resulting in **2.12** in 42% yield. The cyclized product **2.12** was then reacted with 2,4-dimethoxybenzylamine at 140 °C to yield **2.13** (57% yield). 2,4-dimethoxybenzylamine was used instead of benzylamine to allow for more mild deprotection conditions. 40% TFA in DCM was subsequently used to globally deprotect **2.13** to give **2Bxy** in 50% yield.

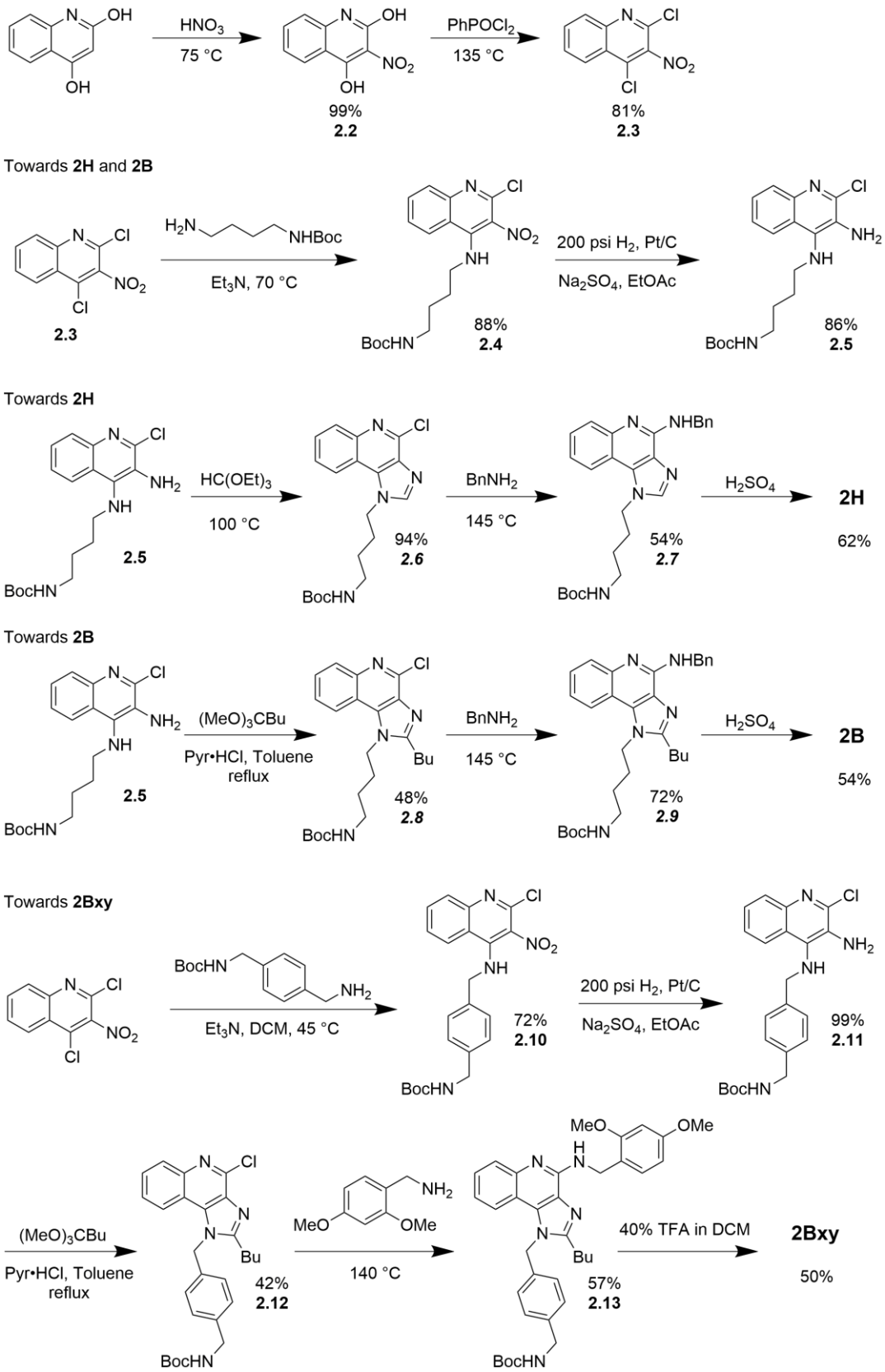

Scheme 2-1: Synthesis of the imidazoquinolines **2H**, **2B**, and **2Bxy**.

2.3 Synthesis of Tosylate Linker and Conjugation to Imidazoquinolines

To make the terminal tosylate linker that would be attached to the imidazoquinolines, 12-hydroxydodecanoic acid **2.14** was esterified under acidic conditions in methanol to yield the methyl ester **2.15** quantitatively (**Scheme 2-2**). Tosylation of the alcohol was then achieved by reaction with tosyl chloride in the presence of pyridine to give **2.16** in 84% yield. Subsequent hydrolysis of the ester with lithium hydroxide in THF and H_2O resulted in the terminal tosylate linker with a carboxylic acid handle, **2.17**, in 94% yield.

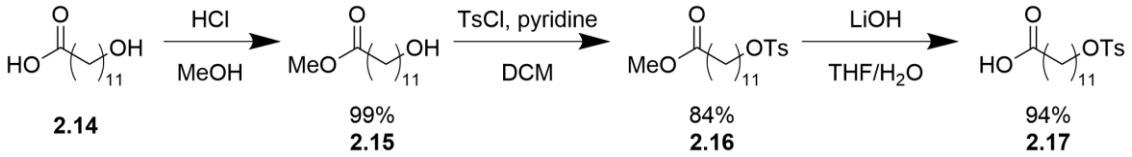

Scheme 2-2: Synthesis of the carboxylic acid functionalized tosylate linker, **2.17**.

We had expected the conjugation of the linker **2.17** with the imidazoquinolines **2H**, **2B**, and **2Bxy** to be trivial, but we were surprised to find that it was actually quite difficult. A variety of coupling reagents, reaction temperatures, and additives were attempted (**Table 2-1**). In most conditions, starting material was consumed, but the reaction yielded unidentifiable products. In conditions without any source of HOBt, HOAt, or DMAP, no reaction was observed. We eventually identified the combination of dicyclohexylcarbodiimide, DCC, with 4-nitrophenol to give the desired conjugation products **2H-OTs**, **2B-OTs**, and **2Bxy-OTs** in low yields (**Scheme 2-3**). We hypothesize that the difficulty of the conjugation was due to competing reactivities in the tosylate and activated carboxylic acid, but we are at a loss as to why the combination of DCC and 4-nitrophenol is the only one we identified to work.

As control compounds, we also synthesized **2H-OH**, **2B-OH**, and **2Bxy-OH** by HATU coupling of **2H**, **2B** and **2Bxy** with 12-hydroxydodecanoic acid in good yields (**Scheme 2-3**).

Table 2-1: Tested conditions for conjugation of **2H** with **2.17** to yield **2H-OTs**

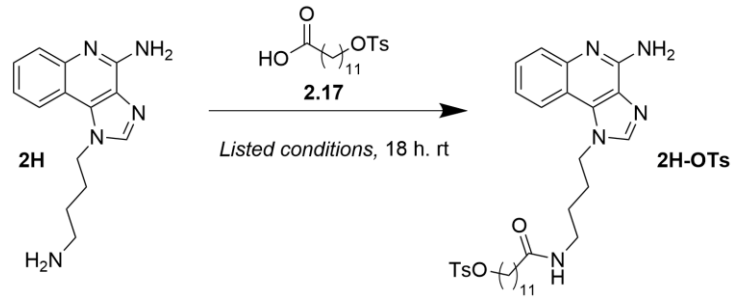

Entry	Coupling Reagent	Additive	Solvent	Temp. (°C)	Reaction Result
1	HATU	-	DMF	20	Unk
2	HATU	HOBt	DMF	20	Unk
3	HATU	DMAP	DMF	20	Unk
4	HATU	-	DMF	40	Unk
5	HATU	-	DCM	20	Unk
6	PyBOP	-	DMF	20	Unk
7	PyBOP	-	DCM	20	Unk
8	PyBOP	HOBt	DCM	20	Unk
9	EDCI	HOBt	DCM	20	Unk
10	EDCI	DMAP	DCM	20	Unk
11	EDCI	HOBt	DMF	20	Unk
12	EDCI	-	DCM	20	NR
13	DCC	-	DCM	20	NR
14	DCC	HOBt	DCM	20	Unk
15	DCC	DMAP	DCM	20	Unk
16	DCC	4-NP	DCM	20	Success

Unk = unknown reaction products; NR = no reaction; Success = 2H-OTs was successfully yielded

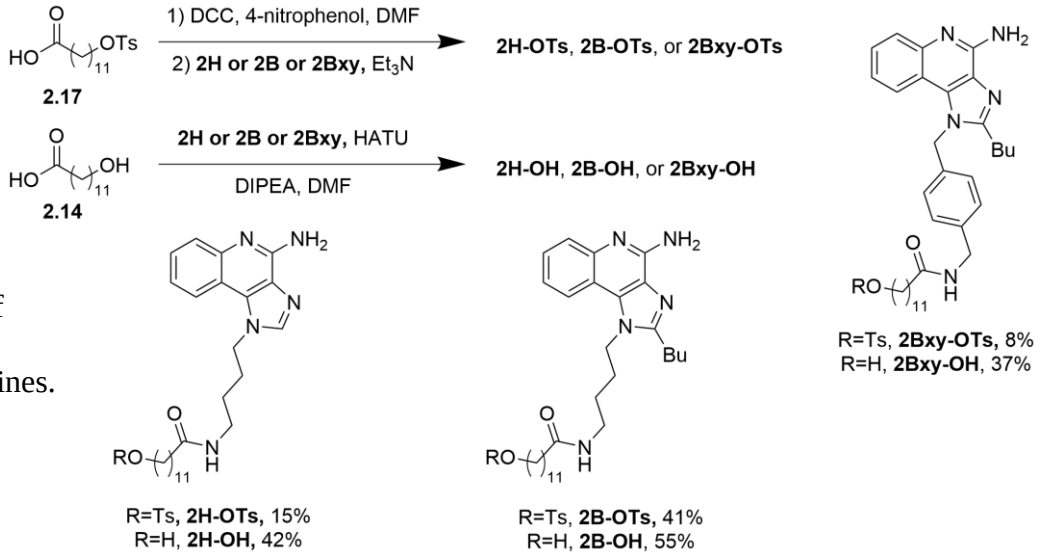

Scheme 2-3: Conjugation of linkers and imidazoquinolines.

2.4 Biological Evaluation of the Covalent Agonists

2.4.1 NF-κB Activity in RAW-Blue Macrophages

With the three covalent agonists and three control agonists in hand we proceeded with incubating our compounds with RAW-Blue macrophages to determine what effect these compounds had on NF-κB activity.

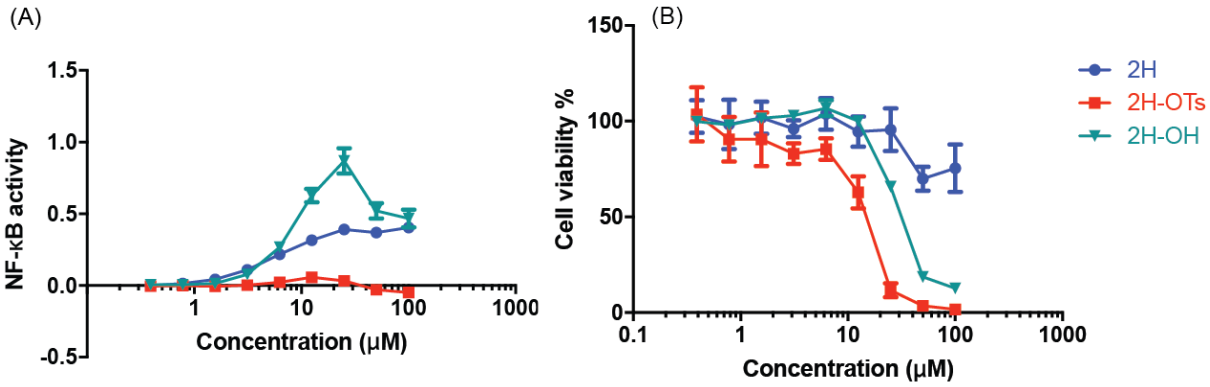

Figure 2-4: Evaluation of **2H**, **2H-OTs**, and **2H-OH** in RAW-Blue macrophages. (A) Normalized NF-κB activity. (B) MTT assay. Each point is an average of three independent experiments. Error bars represent SE.

Looking at the **2H** series of molecules, we can see that three molecules **2H**, **2H-OTs**, and **2H-OH** are quite different in terms of NF-κB activity (**Figure 2-4a**). Relative to **2H**, **2H-OH** results in higher NF-κB activity. Interestingly, **2H-OTs** completely removes NF-κB activity. A MTT assay revealed that there was also more cell death associated with **2H-OTs** than the other compounds (**Figure 2-4b**). The addition of the tosylate clearly altered NF-κB activity and had a negative effect on cell viability. At the higher concentrations, the poor cell viability likely contributed to the non-existent NF-κB activity. This could suggest that covalent modification of the TLR with its agonist resulted in disregulation of the TLR signaling.

In the **2B** series, **2B-OTs** and **2B-OH** exhibit similar dose-dependent NF-κB response, with both resulting in an approximately 3-fold increase in NF-κB activity relative to the parent **2B** (**Figure 2-5a**). In terms of cell viability, all three compounds exhibit good cell viability until the high concentrations (**Figure 2-5b**). These results are quite different from those seen in the **2H** series of compounds. Due to there being little to no difference between **2B-OTs** and **2B-OH**, it is possible that the tosylate is not properly situated to react with a nucleophilic residue due to the addition of the additional butyl chain.

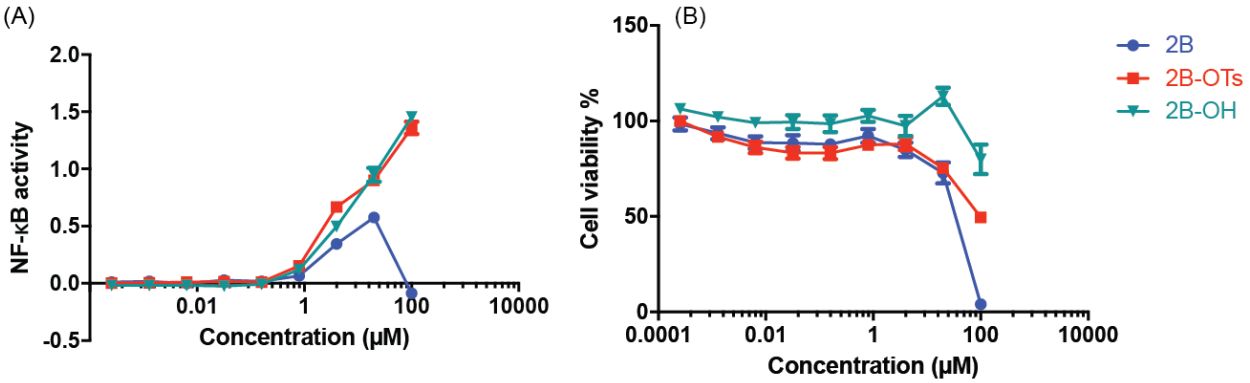

Figure 2-5: Evaluation of **2B**, **2B-OTs**, and **2B-OH** in RAW-Blue macrophages. (A) Normalized NF-**κ**B activity. (B) MTT assay. Each point is an average of three independent experiments. Error bars represent SE.

Similar to **2B**, there were not very large differences in NF-κB activity in the **2Bxy** family of molecules (**Figure 2-6**). There were only minor differences in their EC50. This could suggest that for more potent compounds like **2B** and **2Bxy**, the addition of a linker actually disrupts the initial non-covalent binding of the ligand to the receptor. Additionally, it is possible that due to the added bulk on the molecules, both **2B** and **2Bxy** cannot sit in the receptor binding pocket in a way that would allow for proximity-driven substitution with a nucleophilic side chain to occur.

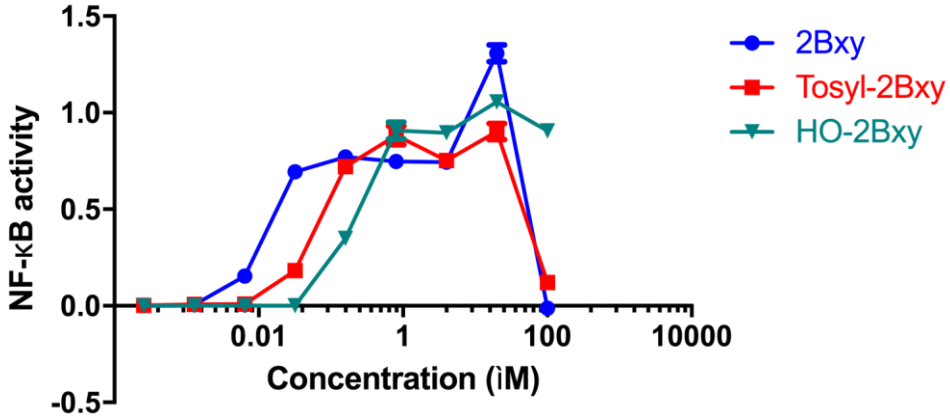

Figure 2-6: Evaluation of **2B**, **2B-OTs**, and **2B-OH** in RAW-Blue macrophages showing normalized NF-**κ**B activity. Each point is an average of three independent experiments. Error bars represent SE.

2.4.2 Cytokine Production in Bone Marrow-derived Dendritic Cells

While the RAW-Blue macrophage NF-κB activity results were quite mixed, we were interested in seeing if these results translated to altered cytokine product in a primary cell line like bone marrow-derived dendritic cells (BMDCs). BMDCs were incubated with 10 μM of each synthesized imidazoquinoline, as well as PBS, LPS, and resiquimod (controls). After 22 h, the supernatant was collected and analyzed by cytometric bead array to determine the output of the cytokines IL-6, MCP-1, IL-10, and TNF-α (**Figure 2-7**). IL-12p70 and IFN-γ were also measured, but none could be detected from the supernatant.

Overall, we can see that **2H-OH** is an outlier and results in much higher cytokine output compared to the other **2H**-derived compounds. The **2H-OH** results correlate well with the increased NF-κB activity seen in the RAW-Blue macrophage assay. Treatment with **2H** and **2H-OTs** appeared to give very similar cytokine outputs.

Treatment with the **2B** and **2Bxy**-derived compounds resulted in subtle differences in cytokine outpu. For IL-10 and TNF-α, there appeared to be no clear trend between treatments with the

parent, **-OTs**, and **-OH** compounds. For both IL-6 and MCP-1, addition of the alkyl linker resulted in decreased cytokine output, regardless of the presence of a tosylate. The NF-κB activities from the RAW-Blue macrophage assay do not seem to be a good indicator of the cytokine outputs of these compounds.

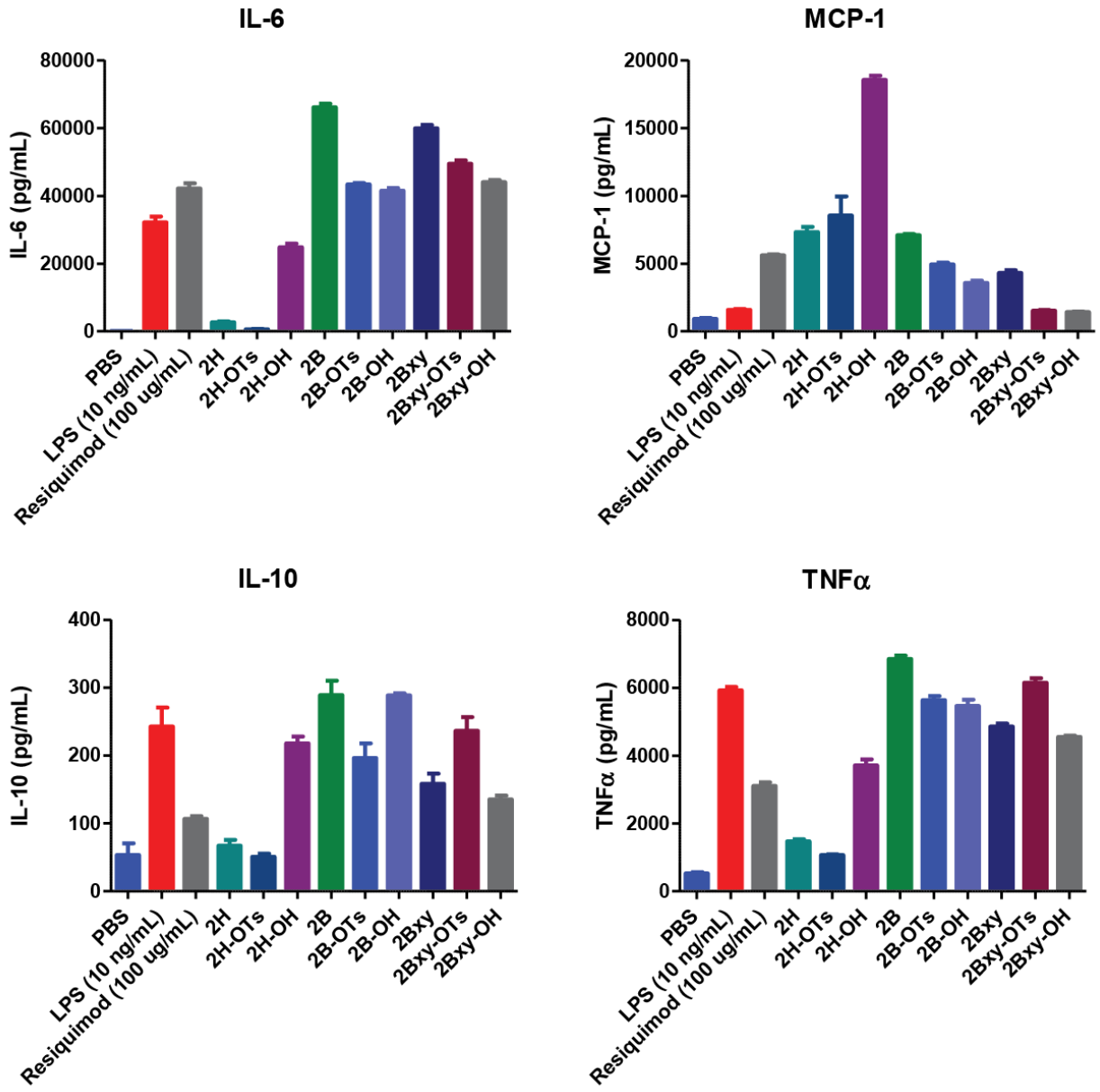

Figure 2-7: BMDC cytokine production determined *via* cytometric bead array. Unless otherwise stated, BMDCs were stimulated with 10 μM of each imidazoquinolines. Average of 3 replicates. Error bars represent SE.

2.4.3 Cytokine Production in Ex Vivo Lymph Node Cultures

One of the objectives we were interested in achieving was improving the pharmacokinetic properties of these imidazoquinolines to elicit a stronger immune response. Thus, working with Geoffrey Lynn (NIH),[8] we evaluated a few of these compounds in murine models.

In our initial experiment, we administered 5 nmol of each compound subcutaneously. After various time points, the proximal lymph node of the mice were harvested and processed to create a cell suspension that was cultured *ex vivo* for 8 h and then evaluated for the presence of IL-12p40 and IP-10 by ELISA (**Figure 2-8**). The **2B** series of compounds were not tested in this experiment.

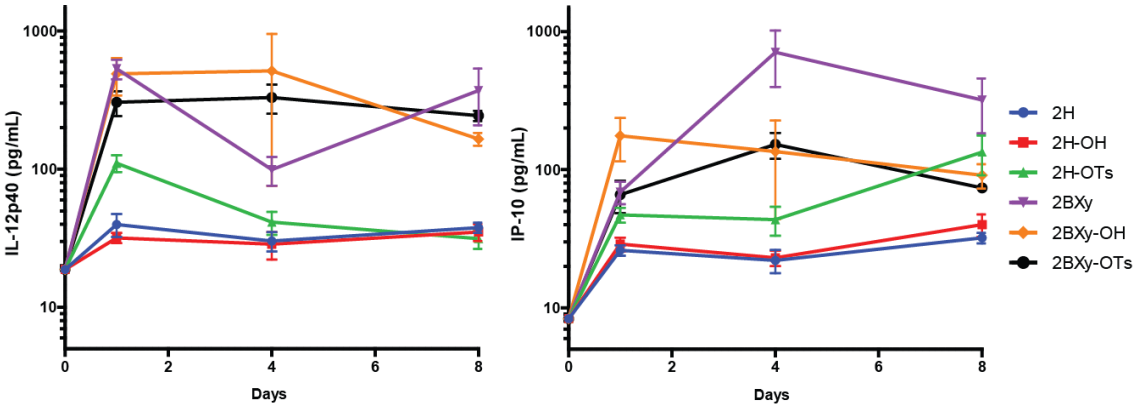

Figure 2-8: E*x vivo* lymph node culture cytokine production measured by ELISA after treatment *in vivo* with 5 nmol of listed imidazoquinolines. N = 4. Error bars represent SE.

Treatment with the **2Bxy** series of compounds did not result in any noticeable differences in cytokine output. This matched our expectations from the NF-κB RAW-Blue macrophage assay. However, treatment with **2H-OTs** resulted in cytokine outputs contradictory to what we had previously observed in other assays. While treatment with **2H** and **2H-OH** were similar to each other, treatment with **2H-OTs** significantly increased the production of both IL-12p40 and IP-10 in the lymph node. This was completely contradictory to the NF-**κ**B activity observed in the RAW-Blue macrophage assay. These results could suggest that there was some sort of

enhancement to the pharmacokinetic properties of the agonists, resulting in an improved immune response *in vivo* versus *in vitro*.

Despite the promising *in vivo* results, we were skeptical and performed a replicate experiment with a new synthetic batch of **2H-OTs** at both 5 nmol and 25 nmol dosages (**Figure 2-9**). During the course of the experiment, it was found that the **2H-OTs** was not well dissolved at high concentrations and precipitated out. This highlighted one of the major disadvantages of using the alkyl linker: poor solubility. We were dismayed to find that the results between this experiment and the previous one were completely different. Treatment with **2H**, **2H-OTs**, and **2H-OH** at two different dosages all resulted in similar cytokine outputs, with no significant differences. A third replication of this experiment also found no significant differences between the treatment groups.

We were unable to ascertain any difference in cytokine output as a result of treatment with our proposed covalent agonist, **2H-OTs**.

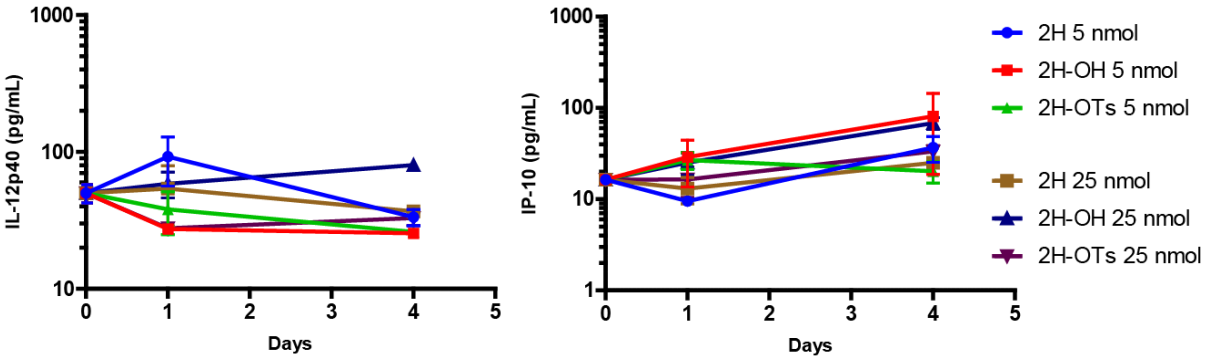

Figure 2-9: E*x vivo* lymph node culture cytokine production measured by ELISA after treatment *in vivo* with 5 or 25 nmol of **2H**, **2H-OTs**, and **2H-OH**. N = 4. Error bars represent SE.

2.5 Determination of Covalent Attachment

2.5.1 Western Blot

Although our biological evaluation of our tosylated imidazoquinoline agonists was troubling, we were interested in knowing if these agonists were actually covalently modifying the receptor. We initially pursued a mass spectrometry approach, but we were unable to isolate enough protein for analysis from cell lysates. In order to improve our isolation yield, we overexpressed TLR8-FLAG in HEK-Blue Null-1-k cells with plasmid from Misako Matsumoto (Hokkaido University Graduate School of Medicine)[9] and subsequently isolated the protein using immunoprecipitation. Unfortunately, this still did not yield an adequate amount of protein for mass spectrometry analysis.

Fortunately, our collaborator for the *in vivo* experiments, Geoffrey Lynn, had developed anti-sera against **2Bxy**,[8] which enabled the ability to use western blot as a method to determine if the covalent agonists were indeed covalently attaching to the TLR.

Three cultures of HEK-Blue Null-1-k cells transiently transfected with TLR8-FLAG were incubated with PBS (one culture, Neg) and 5 μM **2H-OTs** (two cultures). We were curious to see if we could achieve covalent attachment with shorter incubation times with **2H-OTs** and also concerned that we were incubating the cells with the agonist too long. This led us to lyse one of the cultures being treated with **2H-OTs** after only 2 h of incubation. The PBS and other **2H-OTs** treated cultures were lysed after 18 h. All cell lysates were then immunoprecipiated using an anti-FLAG antibody before performing the western blot. Upon labeling with the anti-**2Bxy** sera (primary), biotinylated anti-mouse IgG (secondary), and anti-biotin AlexaFluor650 (tertiary), we were able to observe bands in both **2H-OTs** treated cultures in the expected molecular weight region, ~120 kDa (**Figure 2-10**). No corresponding band was observed in the PBS treated

culture. To ensure that the anti-sera was labeling as intended, a BSA-2H conjugate was synthesized by EDCI coupling and used as a positive control.

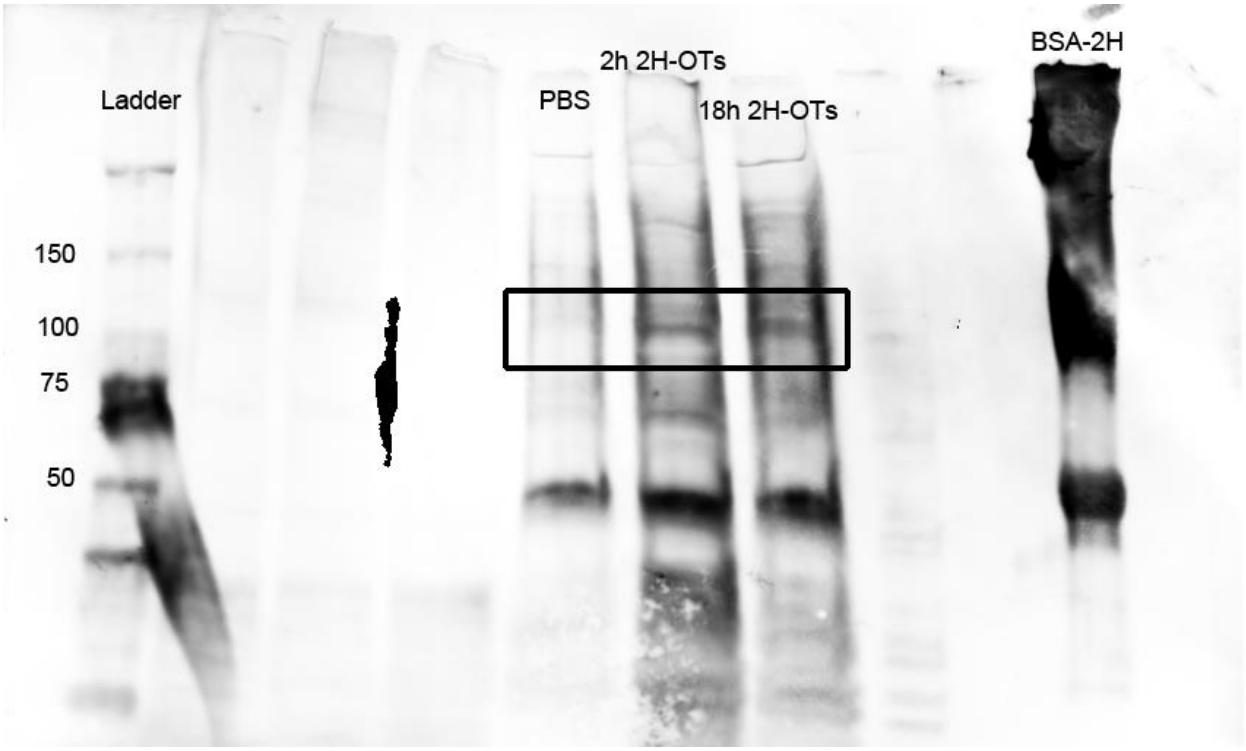

Figure 2-10: Western blot of immunoprecipiated lysates of cells treated with PBS (18 h), **2H-OTs** (2 h), or **2H-OTs** (18 h) to detect covalent modification of TLR 8.

While we were excited about these results, multiplex labeling with anti-FLAG resulted in an oversaturated signal, leading us to be unable to definitively confirm that it was TLR8-FLAG that was being covalently modified or if we were even comparing equal amounts of TLR8-FLAG. Additionally, we did not perform an incubation with **2H** or **2H-OH**, leading us unable to ignore the possibility that it is a non-covalent attachment. However, that seems unlikely given the use of multiple detergents and boiling in Laemmli buffer throughout the lysing and immunoprecipitation steps. These western blot results need to be verified with the proper controls in place.

2.5.2 Synthesis of a Biotinylating TLR 7/8 Probe – Vide Infra

Another approach we are taking to determine if the tosylated agonists are indeed covalently attaching to the receptor is to synthesize TLR 7/8 agonists that will biotinylated the TLR, similar to Hamachi's work with fluorophores and other markers.[4–7] If this probe successfully biotinylates the TLR, it suggest *vide infra* that our covalent agonists are modifying the TLR covalently. This requires the installation of an internal benzene sulfonate into the linker, as opposed to a terminal one.

Synthesis of the biotinylating probe has been more difficult than anticipated. We had originally devised both a linear and convergent route to reach our desired biotinylating TLR 7/8 agonist, but quickly found that the linear route was not feasible due to the amidine making it difficult to install the benzenesulfonate. Thus, we focused our attention on the convergent route (**Scheme 2-4**). In order to best mimic our covalent agonists, we started with 12-aminododecanoic acid (**2.18**) and performed a Fmoc-protection of the amine to provide **2.19**. Subsequent esterification with *tert*-butanol resulted in the fully protected linker **2.20**. We had initially utilized a methyl ester, which was significantly easier to install, but we found that we could not effectively hydrolyze it without also hydrolyzing our benzenesulfonate. Subsequent Fmoc deprotection with piperidine in DMF, followed by reaction with 3-(chlorosulfonyl)benzoyl chloride gives **2.21**. The synthesis is still ongoing, but we anticipate being able to attach the biotin to form the sulfonate and then subsequent acid deprotection to expose the carboxylic acid for conjugation with **2H**.

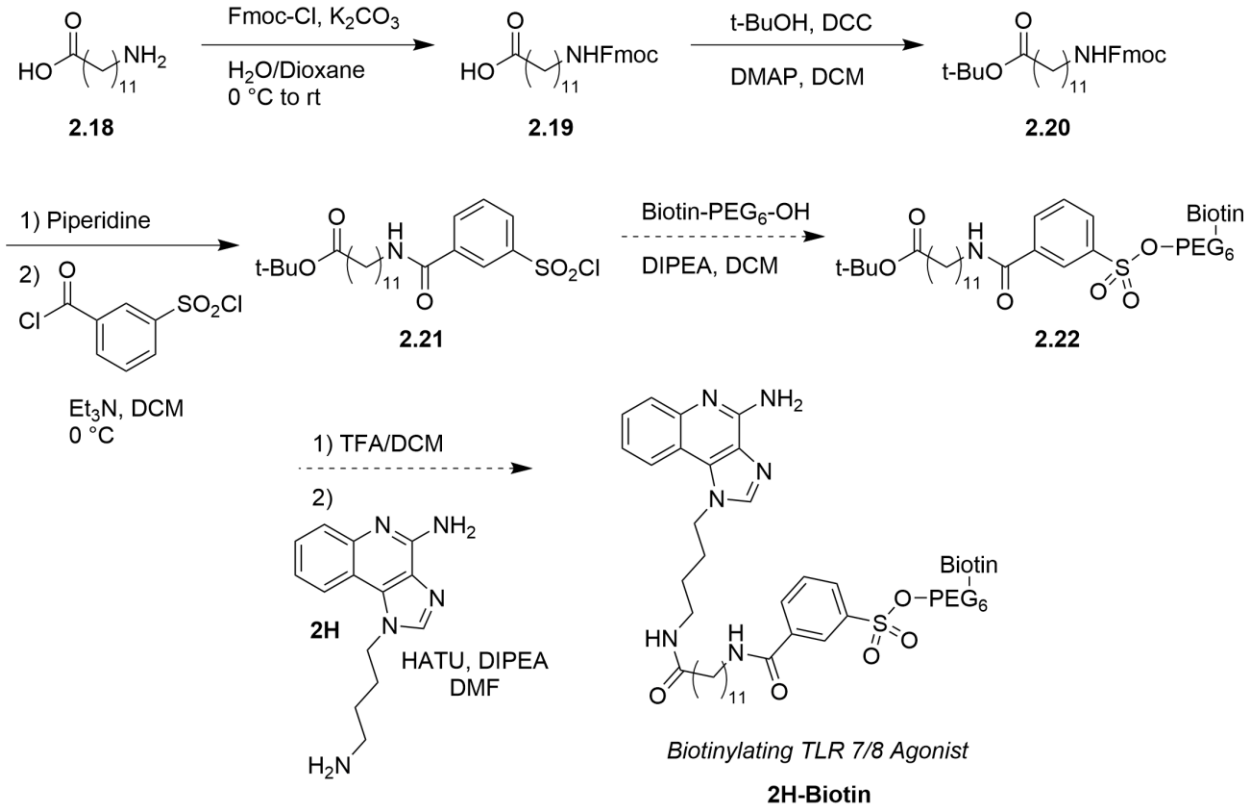

Scheme 2-4: Synthesis towards biotinylating TLR 7/8 agonist.

2.6 Conclusion

We described here the design and synthesis of three potential covalent agonists of TLR 7/8, **2H-OTs**, **2B-OTs**, and **2Bxy-OTs**. *In vitro* studies were performed with these compounds and no clear trend was able to be established for the attachment of the alkyl linker and a tosylate. The most interesting compound so far has been **2H-OTs**, which was the only compound to show a marked difference in NF-**κ**B activity in the RAW-Blue macrophage assay. Initial *in vivo* experiments with **2H-OTs** were promising, but could not be repeated with a separate batch of compound. Efforts are underway towards determining if these covalent agonists are indeed covalently modifying the TLR. In the future, we would like to explore more changes in the linker, particularly in terms of length and type.

2.7 References

(1) Tanji, H.; Ohto, U.; Shibata, T.; Miyake, K.; Shimizu, T. Structural Reorganization of the Toll-Like Receptor 8 Dimer Induced by Agonistic Ligands. *Science* **2013**, *339* (6126), 1426–1429.

(2) Shukla, N. M.; Malladi, S. S.; Mutz, C. A.; Balakrishna, R.; David, S. A. Structure−Activity Relationships in Human Toll-Like Receptor 7-Active Imidazoquinoline Analogues. *J. Med. Chem.* **2010**, *53* (11), 4450–4465.

(3) Yoo, E.; Salunke, D. B.; Sil, D.; Guo, X.; Salyer, A. C. D.; Hermanson, A. R.; Kumar, M.; Malladi, S. S.; Balakrishna, R.; Thompson, W. H.; Tanji, H.; Ohto, U.; Shimizu, T.; David, S. A. Determinants of Activity at Human Toll-like Receptors 7 and 8: Quantitative Structure–Activity Relationship (QSAR) of Diverse Heterocyclic Scaffolds. *J. Med. Chem.* **2014**, *57* (19), 7955–7970.

(4) Tsukiji, S.; Miyagawa, M.; Takaoka, Y.; Tamura, T.; Hamachi, I. Ligand-Directed Tosyl Chemistry for Protein Labeling in Vivo. *Nat. Chem. Biol.* **2009**, *5* (5), 341–343.

(5) Tamura, T.; Tsukiji, S.; Hamachi, I. Native FKBP12 Engineering by Ligand-Directed Tosyl Chemistry: Labeling Properties and Application to Photo-Cross-Linking of Protein Complexes in Vitro and in Living Cells. *J. Am. Chem. Soc.* **2012**, *134* (4), 2216–2226.

(6) Tamura, T.; Kioi, Y.; Miki, T.; Tsukiji, S.; Hamachi, I. Fluorophore Labeling of Native FKBP12 by Ligand-Directed Tosyl Chemistry Allows Detection of Its Molecular Interactions in Vitro and in Living Cells. *J. Am. Chem. Soc.* **2013**, *135* (18), 6782–6785.

(7) Yamaura, K.; Kuwata, K.; Tamura, T.; Kioi, Y.; Takaoka, Y.; Kiyonaka, S.; Hamachi, I. Live Cell off-Target Identification of Lapatinib Using Ligand-Directed Tosyl Chemistry. *Chem. Commun.* **2014**, *50* (91), 14097–14100.

(8) Lynn, G. M.; Laga, R.; Darrah, P. A.; Ishizuka, A. S.; Balaci, A. J.; Dulcey, A. E.; Pechar, M.; Pola, R.; Gerner, M. Y.; Yamamoto, A.; Buechler, C. R.; Quinn, K. M.; Smelkinson, M. G.; Vanek, O.; Cawood, R.; Hills, T.; Vasalatiy, O.; Kastenmüller, K.; Francica, J. R.; Stutts, L.; Tom, J. K.; Ryu, K. A.; Esser-Kahn, A. P.; Etrych, T.; Fisher, K. D.; Seymour, L. W.; Seder, R. A. In Vivo Characterization of the Physicochemical Properties of Polymer-Linked TLR Agonists That Enhance Vaccine Immunogenicity. *Nat. Biotechnol.* **2015**, *33* (11), 1201–1210.

(9) Ishii, N.; Funami, K.; Tatematsu, M.; Seya, T.; Matsumoto, M. Endosomal Localization of TLR8 Confers Distinctive Proteolytic Processing on Human Myeloid Cells. *J. Immunol.* **2014**, *193* (10), 5118–5128.

Chapter 3

Experimental Methods

3.1 General Materials and Methods

The reagents were purchased from Sigma-Aldrich, Alfa Aeser, Acros, or Matrix Scientific and used as is unless otherwise noted. Buffers and media reagents for cell culture were purchased from Fisher Life Technologies. Cytometric Bead Array (CBA) kits were purchased from BD. RAW-Blue and HEK-Blue Null-1-k cell lines were purchased from Invivogen. C57Bl/6 mice were purchased from Jackson Laboratories. pEFBOS-hTLR8-FLAG received *via* a MTA from Misako Matsumoto (Hokkaido University Graduate School of Medicine).[1]

^{1}H and ^{13}C NMR spectra were taken on a CRYO500 (500 MHz) or Avance 600 (600 MHz) spectrometer and analyzed using Topspin or MestreNova software. Spectra are referenced to residual solvent peak for ^{1}HNMR ($CDCl_3$ = 7.26 ppm, MeOD = 3.31 ppm, DMSO = 2.50 ppm) and ^{13}CNMR ($CDCl_3$ = 77.16 ppm, MeOD = 49.00, DMSO = 39.52).[2] Accurate mass spectrometry was performed by the University of California, Irvine Mass Spectrometry Center.

Flash column chromatography was carried out using RediSep Rf normal silica columns on CombiFlash Rf (Teledyne-Isco, Lincoln, NE) instrument unless otherwise mentioned. The solvents were removed under reduced pressure using standard rotary evaporators. Flow cytometry data was acquired using a BD Accuri C6 Flow Cytometer and analyzed using the BD Accuri C6 software. Western blot images were obtained using a GE Typhoon scanner.

3.2 Synthetic Procedures and Characterization

Synthesis of **2.2-2.17, 2H, 2B,** and **2Bxy** were performed according to literature precedent.[3–6] Characterization data of **2.2-2.17, 2H, 2B,** and **2Bxy** have been previously reported.[3–6]

Representative Procedure for the Synthesis of 2H-OTs

To an oven dried 25 mL round bottom flask was added **2.17** (96 mg, 0.26 mmol) and DCC (53 mg, 0.26 mmol), followed by three purges with Ar. The solid was then dissolved in 5 mL anhydrous DCM, followed by the addition of 4-nitrophenol (39 mg, 0.28 mmol). The reaction was left to stir at rt under Ar. After 16 h, the reaction mixture was filtered through a plug of celite into another 25 mL round bottom flask. To the solution was then added **2H** (60 mg, 0.24 mmol) and Et_3N (328 µL, 2.4 mmol). After 12 h, the reaction mixture was diluted with DCM and washed thrice with brine. The aqueous layer was then washed twice with DCM. The combined organic partition was dried over Na_2SO_4, filtered, and concentrated *in vacuo*. The resulting material was column purified (0-10% MeOH in DCM) and lyophilized to yield **2H-OTs** (21 mg, 15%).

2H-OTs

^{1}H NMR (500 MHz, MeOH) δ 8.18 (s, 1H), 8.02 (d, *J* = 8.3 Hz, 1H), 7.82 – 7.71 (m, 3H), 7.61 (d, *J* = 8.3 Hz, 1H), 7.47 (d, *J* = 8.1 Hz, 2H), 7.43 (t, *J* = 7.6 Hz, 1H), 7.25 (t, *J* = 7.6 Hz, 1H), 6.57 (s, 2H), 4.59 (t, *J* = 7.1 Hz, 2H), 3.99 (t, *J* = 6.2 Hz, 2H), 3.06 (q, *J* = 6.6 Hz, 2H), 2.41 (s, 3H), 1.97 (t, *J* = 7.4 Hz, 2H), 1.91 – 1.76 (m, 2H), 1.59 – 1.33 (m, 6H), 1.33 – 1.00 (m, 17H). HRMS (ESI) calcd. for $C_{33}H_{45}N_5O_4SH$ $[M+H]^+$: 608.3270, found: 608.3251.

2B-OTs

^{1}H NMR (600 MHz, MeOD) δ 7.99 (d, *J* = 7.7 Hz, 1H), 7.73 (d, *J* = 8.3 Hz, 2H), 7.67 (d, *J* = 7.5 Hz, 1H), 7.47 (t, *J* = 7.2 Hz, 1H), 7.39 (d, *J* = 8.0 Hz, 2H), 7.33 (t, *J* = 7.1 Hz, 1H), 4.55 – 4.45 (m, 2H), 3.97 (t, *J* = 6.3 Hz, 2H), 3.23 (t, *J* = 6.7 Hz, 2H), 2.97 – 2.89 (m, 2H), 2.41 (s, 3H), 2.08

(t, *J* = 7.5 Hz, 2H), 1.88 (ddt, *J* = 30.8, 15.5, 7.8 Hz, 4H), 1.73 – 1.61 (m, 2H), 1.61 – 1.40 (m, 7H), 1.36 – 1.08 (m, 17H), 1.02 (t, *J* = 7.4 Hz, 3H). ^{13}C NMR (150 MHz, MeOD) δ 176.35, 155.52, 152.56, 146.34, 134.76, 134.59, 131.03, 128.93, 128.45, 126.96, 126.50, 123.74, 121.32, 115.99, 72.02, 46.34, 39.57, 37.14, 30.99, 30.42, 30.41, 30.40, 30.30, 30.25, 30.19, 29.88, 29.82, 28.56, 27.81, 27.56, 26.97, 26.37, 23.57, 21.57, 14.27. HRMS (ESI) calcd. for $C_{37}H_{53}N_5O_4SNa$ $[M+Na]^+$: 686.3716, found: 686.3702.

2Bxy-OTs

^{1}H NMR (500 MHz, MeOH) δ 7.82 (d, *J* = 7.5 Hz, 1H), 7.76 (d, *J* = 8.4 Hz, 2H), 7.66 (d, *J* = 8.3 Hz, 1H), 7.45 – 7.38 (m, 3H), 7.26 (d, *J* = 8.1 Hz, 2H), 7.10 (t, *J* = 7.4 Hz, 1H), 7.03 (d, *J* = 8.1 Hz, 2H), 5.88 (s, 2H), 4.32 (s, 2H), 4.00 (t, *J* = 6.3 Hz, 2H), 3.01 – 2.93 (m, 2H), 2.43 (s, *J* = 12.6 Hz, 3H), 2.18 (t, *J* = 7.4 Hz, 2H), 1.88 – 1.49 (m, 7H), 1.49 – 1.09 (m, 25H), 0.93 (t, *J* = 7.4 Hz, 3H). HRMS (ESI) calcd. for $C_{41}H_{53}N_5O_4SH$ $[M+H]^+$: 712.3896, found: 712.3879.

Representative Procedure for the Synthesis of 2H-OH

To an oven dried 15 mL round bottom flask was added 12-hydroxydodecanoic acid **2.14** (19 mg, 0.086 mmol), **2H** (20 mg, 0.078 mmol), and HATU (33 mg, 0.086 mmol) in 2 mL anhydrous DMF, followed by the addition of DIPEA (27 µL, 0.16 mmol). The reaction was left to stir at rt under Ar. After 16 h, the reaction mixture concentrated *in vacuo*. The resulting material was purified by C18 reverse phase chromatograph (ISCO, 10-90% MeOH in H_2O) and lyophilized to yield **2H-OH** (15 mg, 42%).

2H-OH

^{1}H NMR (500 MHz, MeOH) δ 8.31 (s, 1H), 8.23 (d, *J* = 8.3 Hz, 1H), 7.77 (d, *J* = 8.3 Hz, 1H), 7.72 (t, *J* = 7.7 Hz, 1H), 7.60 (t, *J* = 7.7 Hz, 1H), 4.72 (t, *J* = 7.2 Hz, 2H), 3.53 (t, *J* = 6.6 Hz, 2H), 3.23 (t, *J* = 6.5 Hz, 2H), 2.10 (t, *J* = 7.5 Hz, 2H), 2.05 – 1.93 (m, 2H), 1.70 – 1.56 (m, 2H), 1.50

(dd, *J* = 13.1, 6.5 Hz, 4H), 1.41 – 1.01 (m, 16H). HRMS (ESI) calcd. for $C_{26}H_{39}N_5O_2H$ $[M+H]^+$: 454.3182, found: 454.3190.

2B-OH

^{1}H NMR (500 MHz, $CDCl_3$) δ 8.22 (d, *J* = 8.8 Hz, 1H), 8.03 – 7.94 (m, 1H), 7.77 (d, *J* = 8.7 Hz, 1H), 7.72 (t, *J* = 7.8 Hz, 1H), 7.63 (t, *J* = 7.7 Hz, 1H), 4.64 (t, *J* = 7.9 Hz, 2H), 3.53 (t, *J* = 6.7 Hz, 2H), 3.27 – 3.22 (m, 2H), 3.03 (t, *J* = 7.7 Hz, 2H), 2.11 (t, *J* = 7.4 Hz, 2H), 2.01 – 1.86 (m, 4H), 1.78 – 1.65 (m, 2H), 1.61 – 1.43 (m, 6H), 1.39 – 1.13 (m, 15H), 1.05 (t, *J* = 7.4 Hz, 3H). ^{13}C NMR (150 MHz, MeOD) δ 178.38, 176.41, 151.81, 144.39, 140.93, 131.38, 129.75, 129.00, 126.43, 122.65, 122.03, 116.12, 62.99, 49.43, 49.28, 49.14, 49.00, 48.86, 48.72, 48.57, 46.96, 39.53, 37.81, 37.13, 33.65, 30.72, 30.69, 30.65, 30.62, 30.58, 30.53, 30.45, 30.43, 30.34, 30.24, 30.15, 28.17, 27.93, 27.45, 27.00, 26.93, 25.73, 23.44, 14.26. HRMS (ESI) calcd. for $C_{30}H_{47}N_5O_2H$ $[M+H]^+$: 510.3808, found: 510.3825.

2Bxy-OH

^{1}H NMR (500 MHz, $CDCl_3$) δ 7.95 (d, *J* = 7.8 Hz, 1H), 7.73 (d, *J* = 8.1 Hz, 1H), 7.61 (dd, *J* = 15.3, 7.9 Hz, 1H), 7.34 (t, *J* = 7.4 Hz, 1H), 7.28 (d, *J* = 8.2 Hz, 2H), 7.05 (d, *J* = 8.2 Hz, 2H), 5.93 (s, 2H), 4.32 (s, 2H), 3.53 (t, *J* = 6.7 Hz, 2H), 3.05 – 2.96 (m, 2H), 2.19 (t, *J* = 7.4 Hz, 2H), 1.92 – 1.75 (m, 2H), 1.71 – 1.17 (m, 28H), 0.94 (t, *J* = 7.4 Hz, 3H).

3.3 Biological Testing

RAW-Blue (RAW264.7) Macrophage NF-κB Assay

RAW-Blue cells were plated at 55 × 10^4 cells/mL density (180 μL) in 96-well plates using testing media: D-MEM High Glucose medium (Life Technologies), 10% heat inactivated FBS, 2 mM L-glutamine, and antibiotic-antimycotic (1x). RAW-Blue cells were incubated with 20 μL of each

treatment for 18 h at 37 °C in a CO_2 incubator. Cell medium (50 μL) from the stimulated RAW-Blue cells was removed, placed into a 96-well plate, and incubated with QUANTI-Blue solution (InvivoGen) (150 μL) for 1 h at 37 °C in a CO_2 incubator. The absorbance (620 nm) was measured using a Fisher Scientific MultiSkan FC.

Bone Marrow-Derived Dendritic Cell (BMDC) Harvest and Culture

Bone marrow-derived dendritic cells (BMDCs) were harvested from 6-week-old C57Bl/6 mice (Jackson Laboratory). Femur bones were removed from mice according to protocols described by Matheu,[7] and the bone marrow was extracted into PBS buffer. The cell suspension was made into a homogeneous solution using a pipette, and subsequently filtered through a 70 μm cell strainer. The cell solution was centrifuged at 300 rcf for 10 min at RT. The supernatant was removed, and ACK Lysing Buffer (3 mL, Lonza) was added to the cell pellet and incubated for 3 min at RT. PBS buffer (12 mL) was then added to the cell suspension, and the cell solution was centrifuged at 300 rcf for 10 min at RT. In a washing step, the cell pellet was suspended in RPMI 1640 (Fisher Scientific) and centrifuged at 300 rcf for 10 min at RT. Thereafter, the cell pellet was resuspended in BMDC complete media. Harvested cells were plated at $1x10^6$cells/mL in 100 mm Petri dishes (10 mL total media) and incubated at 37 °C in 5% CO_2 (day 0 of cell culture). On day 3, 10 mL of fresh BMDC primary media was added to each Petri dish. On day 5, BMDCs were released by repeated pipetting, centrifuged at 300 RCF for 10 min at RT, suspended in DMEM complete media.

General Procedure for BMDC Stimulation and Cytokine Measurement by CBA

BMDCs were plated at at 500k cells/0.45 mL in 24-well plates using culture media. BMDCs were incubated with 50 μL of each treatment for 18 h at 37 °C with 5% CO_2. The cells were released from the plate and transferred to microcentrifuge tubes. The cells were centrifuged at 300 RCF at

rt for 10 min. The supernatant was then diluted 5x and used for cytometric bead array (CBA) according to manufacturer's instructions.

Ex vivo lymph node cultures for cytokine determination (with Geoffrey Lynn, NIH)[3]

Treatments were prepared in sterile, endotoxin-free PBS (Gibco, Life Technologies) and administered subcutaneously in a total volume of 50 µL. Proximal draining lymph nodes were harvested at various time points following subcutaneous administration of different treatments and placed in 300 µL of RPMI supplemented with 10% (v/v) FCS, 50 U/mL penicillin, 50 µg/mL streptomycin, and 2 mM L-gluatmine in 1.5 mL DNase, RNase, Pyrogen free Kontes Pellet Pestle Grinders (Kimble-Chase, Vineland, NJ) sitting on ice. Lymph nodes were gently mechanically disrupted using sterile pestles and the resulting suspensions were vortexed for 5 s and added to a 96 well round bottom culture plate that was incubated at 37 °C/5% CO_2 for 8 h. Supernatant was the collected and stored at -80 °C until analyzed by ELISA. ELISA kits for murine IL-12p40 and IP-10 were obtained from Peprotech (Rocky Hill, NJ).

Transfection, Immunoprecipitation, and Western Blot

HEK-Blue Null-1-k cells (Invivogen) cultured in 10 cm petri dishes (3 x 10^6 cells/dish) were transfected with pEFBOS-hTLR8-FLAG (Misako Matsumoto, Hokkaido University Graduate School of Medicine)[1] using FuGENE HD (Roche). 20 h after transfection, cells were replated in 10 cm dishes and incubated with PBS or agonists.

After desired length of incubation time, cells were lysed in NP-40 lysis buffer (1% NP-40, 150 mM NaCl, 50 mM pH 8 Tris-Cl, and protease inhibitor cocktail) for 10 min at 4 °C. The lysates were sonicated 3 x 10 sec, followed by 20 min at 4 °C. Then lysates were centrifuged at 14000 xg at 4 °C for 10 min. To the lysates was added 2 µg anti-FLAG Rabbit mAb and 50 µL of Protein A Microbeads (Miltenyi Biotec). After mixing well, the mixture was left to incubate on ice for 30

min. The lysates were passed through the µ Column (Miltenyi Biotec), rinsed 4x200 µL with NP-40 lysis buffer, rinsed 1x100 µL with 20 mM pH 8 Tris-Cl, and eluted with pre-heated 1x Laemmli Buffer (Bio-Rad).

Samples were analyzed by SDS-PAGE (4-15% gel) under reducing conditions, followed by transfer onto a low fluorescence-PVDF (Bio-Rad). Subsequent immunoblotting was performed with anti-2Bxy sera (Geoffrey Lynn, NIH), biotinylated anti-mouse IgG, and anti-biotin AlexaFluor650.

3.4 References

(1) Ishii, N.; Funami, K.; Tatematsu, M.; Seya, T.; Matsumoto, M. Endosomal Localization of TLR8 Confers Distinctive Proteolytic Processing on Human Myeloid Cells. *J. Immunol.* **2014**, *193* (10), 5118–5128.

(2) Fulmer, G. R.; Miller, A. J. M.; Sherden, N. H.; Gottlieb, H. E.; Nudelman, A.; Stoltz, B. M.; Bercaw, J. E.; Goldberg, K. I. NMR Chemical Shifts of Trace Impurities: Common Laboratory Solvents, Organics, and Gases in Deuterated Solvents Relevant to the Organometallic Chemist. *Organometallics* **2010**, *29* (9), 2176–2179.

(3) Lynn, G. M.; Laga, R.; Darrah, P. A.; Ishizuka, A. S.; Balaci, A. J.; Dulcey, A. E.; Pechar, M.; Pola, R.; Gerner, M. Y.; Yamamoto, A.; Buechler, C. R.; Quinn, K. M.; Smelkinson, M. G.; Vanek, O.; Cawood, R.; Hills, T.; Vasalatiy, O.; Kastenmüller, K.; Francica, J. R.; Stutts, L.; Tom, J. K.; Ryu, K. A.; Esser-Kahn, A. P.; Etrych, T.; Fisher, K. D.; Seymour, L. W.; Seder, R. A. In Vivo Characterization of the Physicochemical Properties of Polymer-Linked TLR Agonists That Enhance Vaccine Immunogenicity. *Nat. Biotechnol.* **2015**, *33* (11), 1201–1210.

(4) Chiang, C.-H.; Ramu, R.; Tu, Y.-J.; Yang, C.-L.; Ng, K. Y.; Luo, W.-I.; Chen, C. H.; Lu, Y.-Y.; Liu, C.-L.; Yu, S. S.-F. Regioselective Hydroxylation of C12–C15 Fatty Acids with Fluorinated Substituents by Cytochrome P450 BM3. *Chem. – Eur. J.* **2013**, *19* (41), 13680–13691.

(5) Sakai, T.; Kawai, H.; Kamishohara, M.; Odagawa, A.; Suzuki, A.; Uchida, T.; Kawasaki, T.; Tsuruo, T.; Otake, N. Structure-Antitumor Activity Relationship of Semi-Synthetic Spicamycin Derivatives. *J. Antibiot. (Tokyo)* **1995**, *48* (12), 1467–1480.

(6) Shukla, N. M.; Malladi, S. S.; Mutz, C. A.; Balakrishna, R.; David, S. A. Structure−Activity Relationships in Human Toll-Like Receptor 7-Active Imidazoquinoline Analogues. *J. Med. Chem.* **2010**, *53* (11), 4450–4465.

(7) Matheu, M. P.; Sen, D.; Cahalan, M. D.; Parker, I. Generation of Bone Marrow Derived Murine Dendritic Cells for Use in 2-Photon Imaging. *JoVE J. Vis. Exp.* **2008**, No. 17, e773–e773.

Appendix

NMR Spectra

2H-OTs

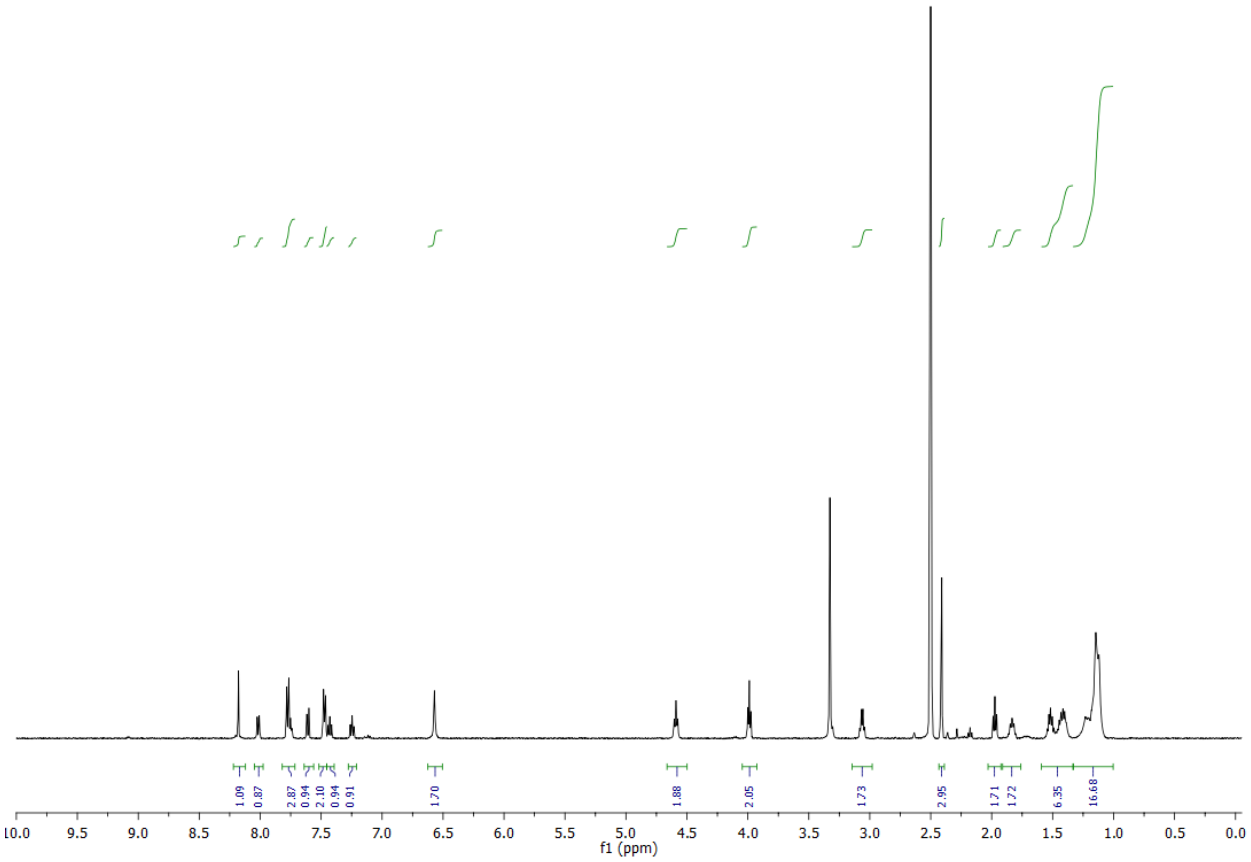

2B-OTs

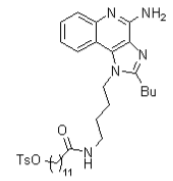
NH2
N
N
Bu
O
N
H
TsO
11

1.00
1.94
1.04
1.06
1.95
1.03
1.91
1.87
1.92
1.89
2.83
1.96
3.99
2.11
6.57
16.21
3.05
f1 (ppm)

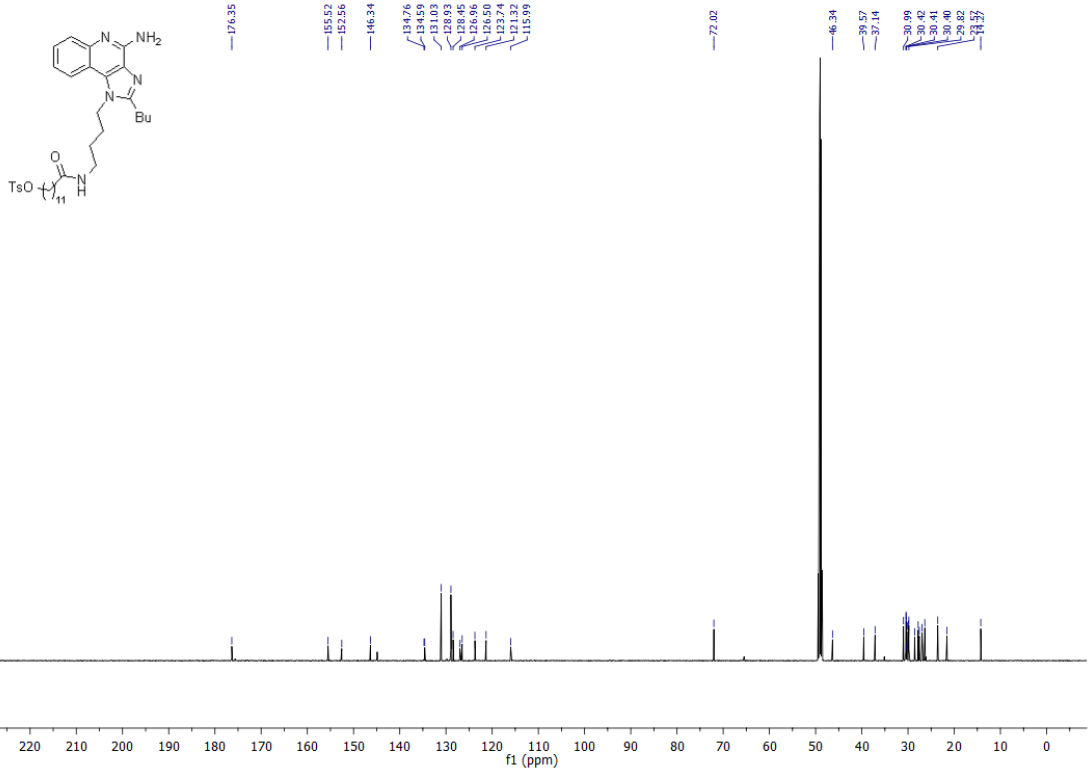
176.35
155.52
152.56
146.34
134.76
134.59
131.03
128.93
126.96
126.50
123.74
121.32
115.99
72.02
46.34
39.57
37.14
30.99
30.42
30.41
30.40
29.82
23.57
14.27
f1 (ppm)

2Bxy-OTs

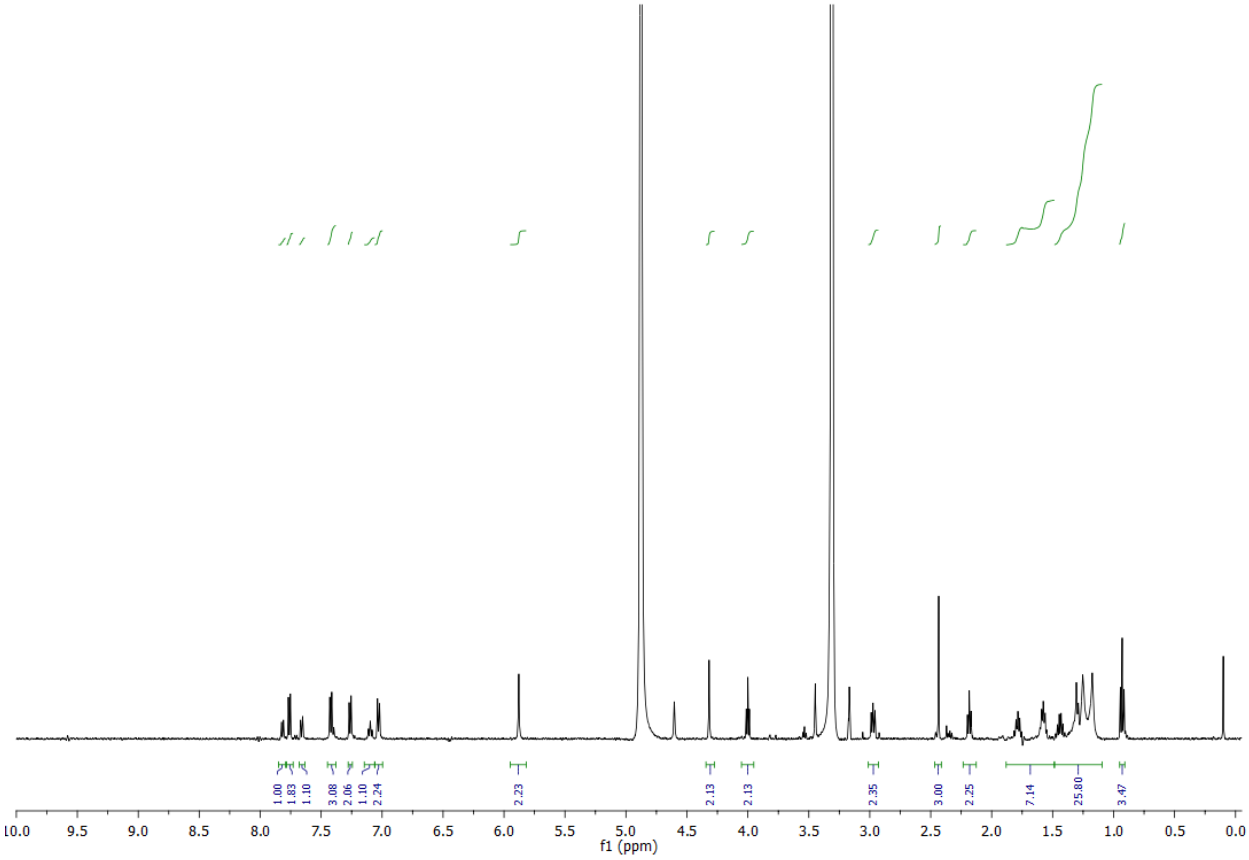
1.00
1.83
1.10
3.08
2.06
1.10
2.24
2.23
2.13
2.13
2.35
3.00
2.25
7.14
25.80
3.47
10.0
9.5
9.0
8.5
8.0
7.5
7.0
6.5
6.0
5.5
5.0
4.5
4.0
3.5
3.0
2.5
2.0
1.5
1.0
0.5
0.0
f1 (ppm)

2H-OH

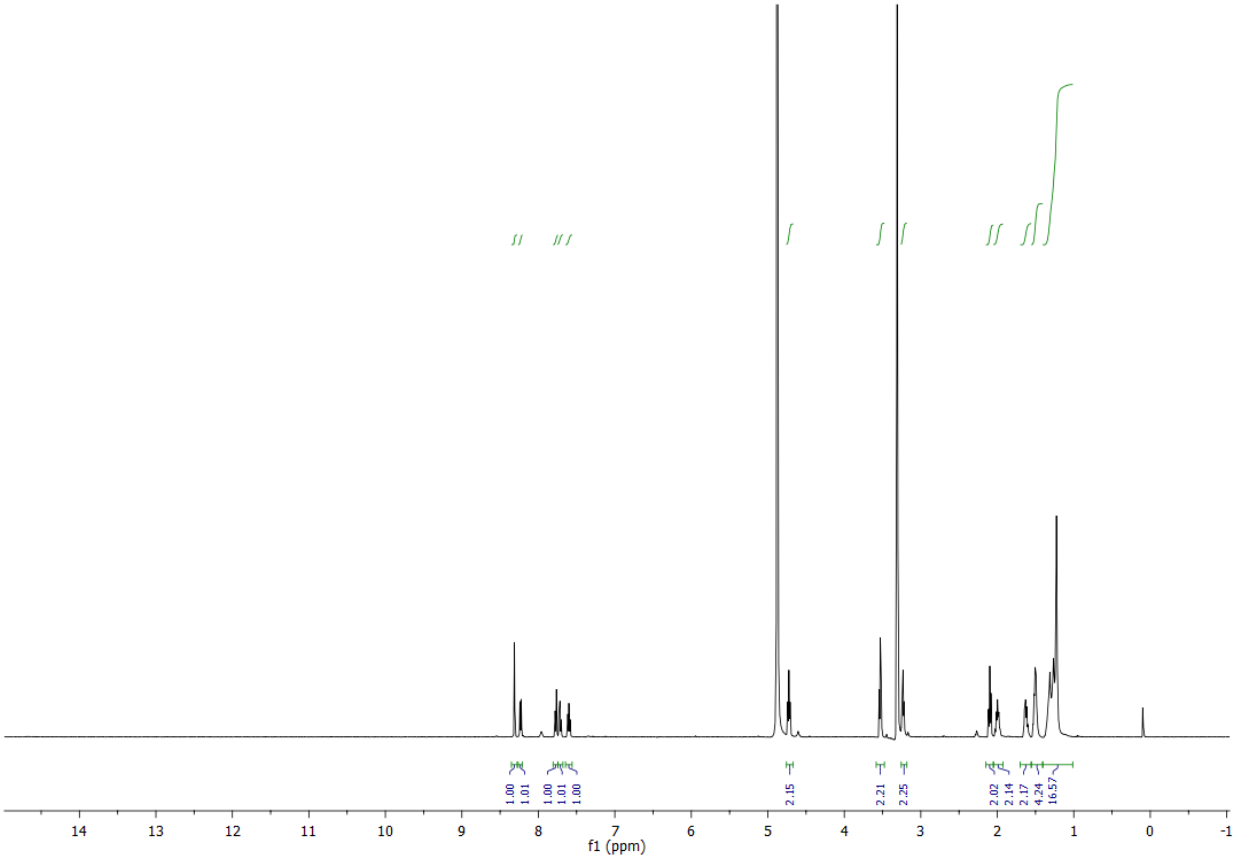
1.00
1.01
1.00
1.01
1.00
2.15
2.21
2.25
2.02
2.14
2.17
4.24
16.57
14
13
12
11
10
9
8
7
6
5
4
3
2
1
0
-1
f1 (ppm)

2B-OH

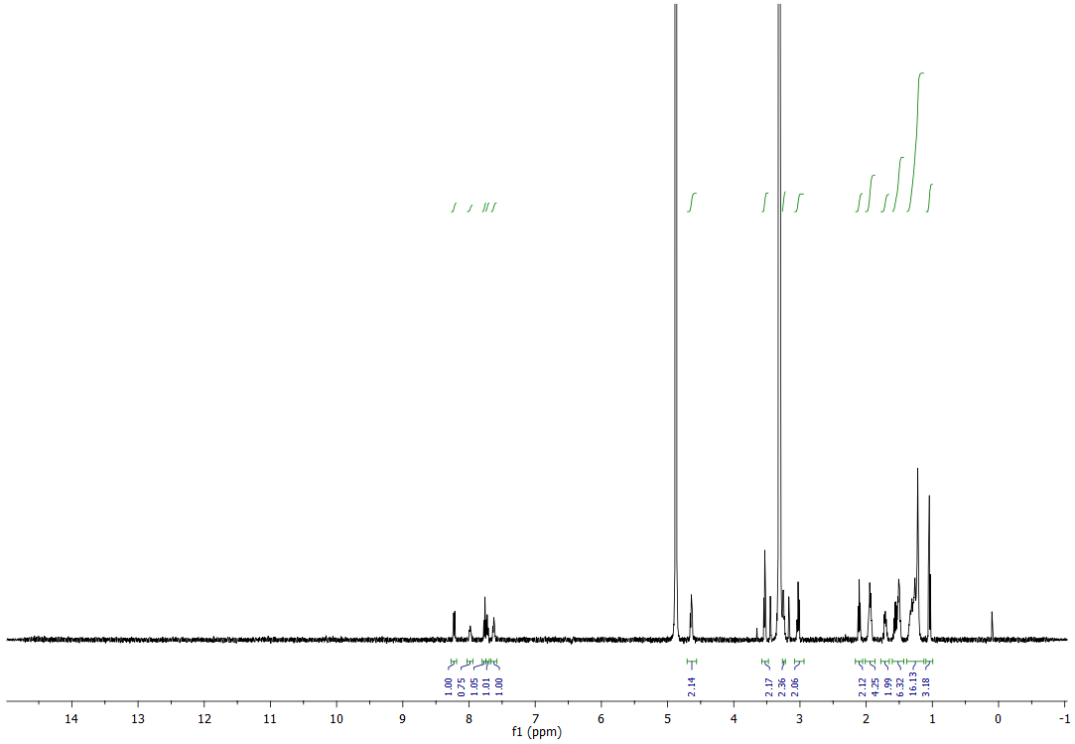
1.00
0.75
1.05
1.01
1.00
2.14
2.17
2.36
2.06
2.12
4.25
1.99
6.32
16.13
3.18
f1 (ppm)

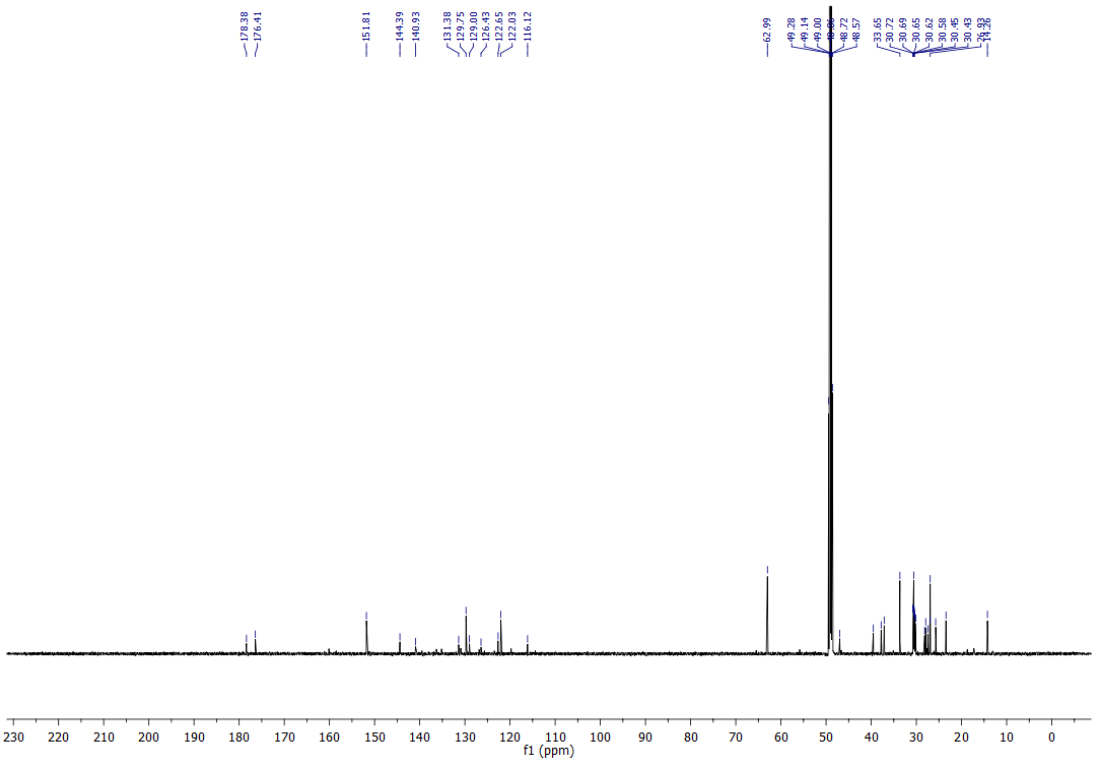
178.38
176.41
151.81
144.39
140.93
131.38
129.75
129.00
126.43
123.65
122.03
116.12
62.99
49.28
49.14
49.00
48.72
48.57
33.65
30.72
30.69
30.65
30.62
30.58
30.45
30.43
f1 (ppm)

2Bxy-OH

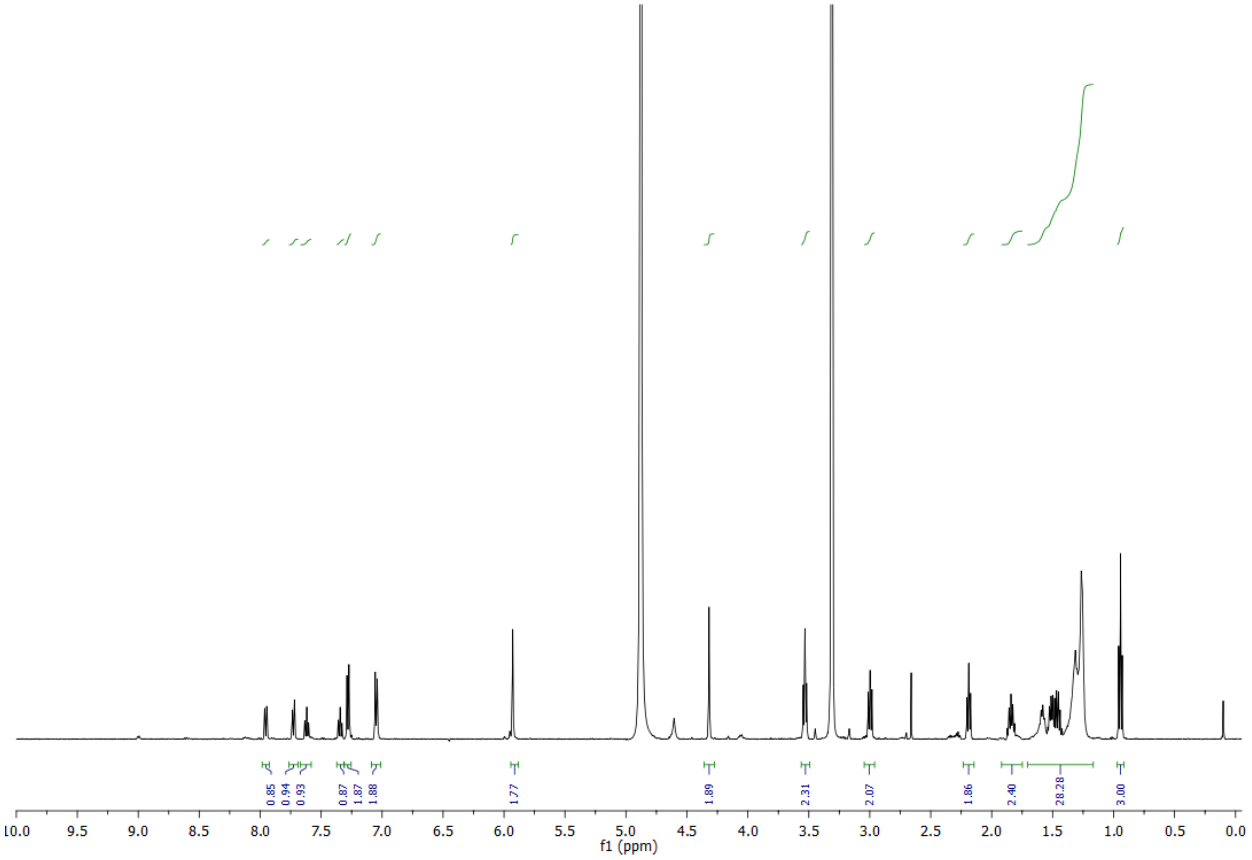
0.85
0.94
0.93
0.87
1.87
1.88
1.77
1.89
2.31
2.07
1.86
2.40
28.28
3.00
10.0
9.5
9.0
8.5
8.0
7.5
7.0
6.5
6.0
5.5
5.0
4.5
4.0
3.5
3.0
2.5
2.0
1.5
1.0
0.5
0.0
f1 (ppm)